The EUMETSAT Network of Satellite Application Facilities

NWP SAF
Numerical Weather Prediction

Document NWPSAF-MO-TR-029

Version 1.0

13/03/14

# NWP SAF AMV monitoring: the 6th Analysis Report (AR6)

James Cotton

Met Office, UK

Met Office

ECMWF

Royal Netherlands Meteorological Institute
Ministry of Transport, Public Works and Water Management

METEO FRANCE
Toujours un temps d'avance

**NWP SAF AMV monitoring: the 6th Analysis Report (AR6)**

James Cotton

Met Office, UK

This documentation was developed within the context of the EUMETSAT Satellite Application Facility on Numerical Weather Prediction (NWP SAF), under the Cooperation Agreement dated 29 June 2011, between EUMETSAT and the Met Office, UK, by one or more partners within the NWP SAF. The partners in the NWP SAF are the Met Office, ECMWF, KNMI and Météo France.



| Change record | | | |
|---|---|---|---|
| Version | Date | Author / changed by | Remarks |
| 0.1 | 31/01/14 | J Cotton | First draft |
| 0.2 | 03/03/14 | J Cotton | Minor updates following comments from Mary Forsythe. Added extra plots for Feature 3.2. |
| 1.0 | 13/03/14 | J Cotton | Version for publication |
| | | | |

## Contents

## 1. Introduction

The NWP SAF (Satellite Application Facility for Numerical Weather Prediction) atmospheric motion vector (AMV) monitoring, http://research.metoffice.gov.uk/research/interproj/nwpsaf/satwind_report/index.html, aims to help characterise AMV errors in order to aid improvements to the AMV derivation and their treatment in NWP models. One of the ways this can be achieved is via long term monitoring of trends and patterns in observed minus background (O-B) statistics. The AMVs are compared with short-range forecasts from an NWP model, valid at the same time and location as the observation. The NWP SAF maintains an archive of O-B statistics against both the Met Office and ECMWF global model backgrounds, providing a framework in which we can attempt to separate error contributions. Differences between centres suggest model-dependent problems whereas similarities suggest either problems with the AMVs or problems shared by the models.

The NWP SAF O-B monitoring hosts a wealth of information for different satellites, channels and AMV producers and to exploit this resource requires a comprehensive and thorough investigation. This is where the AMV *analysis reports* (AR) come in. These reports, now published every 2 years, attempt to summarise the main features identified in the O-B monitoring and record how they have evolved over time as updates are made to the AMV derivation and the NWP systems. Where possible, an attempt is made to diagnose the cause of the observed bias using tools such as model best-fit pressure and comparison to other wind and cloud top height products. This document marks the sixth entry in the series of analysis reports (AR6). Previous analysis reports are hereafter referred to as AR5 (2012), AR4 (2010), AR3 (2008), AR2 (2005) and AR1 (2001) and are available to download from the website.

The status of the AMV monitoring as of January 2014 is given in Table 1. Changes to the monitoring since AR5 are listed in Table 2. There have also been significant updates to some existing data sets:

1. **EUMETSAT CCC scheme**. The EUMETSAT MSG AMV processing was updated on 5 September 2012 to make use of the Cross Correlation Contribution (CCC) method (Borde and Oyama, 2008). The new scheme maintains a closer link between the pixels used in the height assignment with those that dominate in the tracking. Where appropriate, the impact of the CCC scheme is addressed within the separate features of this report. Briefly, the use of CCC has resulted in some significant improvements e.g. a reduction of the negative speed bias at high level

in the jet regions which had been a persistent and growing problem for the MSG winds (ref. Feature 2.10 in AR5). However, a degradation in the statistics was observed for the low level (below 700 hPa) IR and visible winds (see Borde et al., 2013). An update to the low level AMV processing has subsequently been implemented in EUMETSAT operations on 16 April 2013.

2. **EUMETSAT Metop winds**. Several updates have been made to the EUMETSAT polar system including the introduction of height assignment using IASI in April 2012.

3. **GOES hourly winds**. As discussed in AR5, the GOES AMV processing was expected to be updated in the first half of 2012. In AR5, the investigation of features using GOES data made use of a test hourly winds dataset and subsequently some features were declared as 'fixed'. However, the implementation of the hourly winds has been delayed and as of January 2014 a date has yet to be decided. Features previously identified as being fixed in AR5 will remain so in AR6.

| **Geostationary AMVs** | **Channels** | **Polar AMVs** | **Channels** |
|---|---|---|---|
| Meteosat-10 | IR 10.8, WV 6.2, WV 7.3, VIS 0.8, HRVIS | Terra (CIMSS, NESDIS, DB) | IR, WV, CSWV |
| Meteosat-9 | IR 10.8, WV 6.2, WV 7.3, VIS 0.8, HRVIS | Aqua (CIMSS, NESDIS, DB) | IR, WV, CSWV |
| Meteosat-7 | IR, WV, VIS | NOAA-15 (CIMSS) | IR |
| Kalpana | IR, WV | NOAA-16/18/19 (CIMSS, DB) | IR |
| FY-2E | IR, WV | Metop-A (EUMETSAT, CIMSS) | IR |
| MTSAT-1R/2 | IR, WV, VIS | Metop-B (EUMETSAT, CIMSS) | IR |
| GOES-15 (+unedited) | IR 10.7, IR 3.8, WV, VIS | **Mixed AMVs** | **Channels** |
| GOES-13 (+unedited) | IR 10.7, IR 3.8, WV, VIS | LeoGeo (CIMSS) | IR |

**Table 1. AMV datasets monitored by the NWP SAF. DB = direct broadcast, IR = infrared, VIS = visible, HRVIS = high resolution VIS, WV = cloudy water vapour, CSWV = clear sky WV.**

| **Change** | **Type** | **Date** | **Description** |
|---|---|---|---|
| Meteosat-10 | Transition | 21/01/13 | Meteosat-10 (MSG-3) replaced Meteosat-9 at 0° |
| Meteosat-9 | Transition | 04/04/13 | Replaced Meteosat-8 for rapid scan winds at 9.5°E |
| Meteosat-8 | Removed | 04/04/13 | No longer monitored |
| FY-2E | New | 05/12 | Added to monitoring (data Jan 2011 onwards) |
| Kalpana | New | 12/13 | Added to monitoring (data Oct 2013 onwards) |
| LeoGeo | New | 03/12 | Added to monitoring (data Jan 2012 onwards) |
| Metop-B | New | 01/13 | Added CIMSS winds (data Jan 2013 onwards) |
| Metop-B | New | 04/13 | Added EUMETSAT winds (data Apr 2013 onwards) |
| Terra WV | Removed | 25/07/13 | Terra WV AMVs no longer produced - striping/noise |

**Table 2. Changes since AR5.**

The report is structured as follows. Section 2 gives an overview of the current active features identified in the monitoring statistics. Sections 3, 4 and 5 then present relevant updates to these features for low level (below 700 hPa), mid level (400-700 hPa) and high level (above 400 hPa) AMVs respectively. The polar AMVs are addressed separately in section 6, followed by a short summary in section 7.

## 2. Index of features

Following the convention of previous reports, features are referenced X.Y, where X is the number of the analysis report where the feature was first described and Y is the example number. Unless otherwise specified, the tropics refer to the area 20°N-20°S and the extra-tropics polewards of these boundaries. Table 3 summarises the status of each feature and indicates whether further information is provided in this report. In some cases features may have been renamed to better reflect the pattern or cause.

| Ref. | Feature | AR | Resolved? | Update ? |
|---|---|---|---|---|
| **Low level (below 700 hPa)** | | | | |
| 2.1 | GOES fast bias in inversion regions | 2,3,5 | Fixed in new product | N |
| 2.3 | GOES winter negative bias over NE America | 2,3 | Improved in new product over sea | Y |
| 2.6 | MSG positive bias over N Africa | 2,3,4 | No | Y |
| 2.7 | Spuriously fast Meteosat and MTSAT winds | 2,3,4 | No | Y |
| 4.1 | Model differences in the Pacific | 4,5 | No | N |
| 5.1 | Patagonia negative bias | 5 | No | N |
| 5.2 | MSG negative bias during Somali Jet | 5 | No | Y |
| 6.1 | Bias in tropical E Atlantic | new | new | Y |
| 6.2 | MTSAT and FY-2E bias during NE winter monsoon | new | new | Y |
| **Mid level (400-700 hPa)** | | | | |
| 2.8 | Positive bias in the tropics | 2,3,4,5 | No | Y |
| 2.9 | Negative bias in the extra-tropics | 2,3,4,5 | MSG improved | Y |
| **High level (above 400 hPa)** | | | | |
| 2.10 | Jet region negative speed bias | 2,3,4,5 | MSG improved | Y |
| 2.13 | Tropics positive speed bias | 2,3,4,5 | MSG improved | Y |
| 2.14 | High troposphere positive bias | 2,3 | No | Y |
| 2.15 | Differences between channels | 2,3,5 | Covered within features | N |
| 3.2 | Negative speed bias in TEJ | 3 | No | Y |
| 3.3 | GOES-W bias change at 180° | 3,5 | Fixed in new product | Y |
| 4.2 | GOES negative bias in tropical Pacific | 4,5 | No | Y |
| 5.3 | MTSAT tropical cyclone speed bias | 5 | No | Y |
| 6.3 | Very high FY-2E WV winds | new | No | Y |
| **Polar AMVs** | | | | |
| 2.19 | High level positive speed bias | 2,3,4,5 | No | N |
| 2.20 | Low level negative speed bias | 2,3,4 | No | N |
| 3.6 | NESDIS-CIMSS polar AMV differences | 3,5 | No longer significant - close | N |
| 4.3 | Near-pole mid level negative bias | 4,5 | No | N |
| 6.4 | EUMETSAT Metop near the poles | new | No | Y |

**Table 3. Status of the current features identified in the AMV monitoring. Green shading denotes a new feature, blue denotes a feature than is fixed or considered closed.**

## 3. Low level updates

### Feature 2.3. GOES winter negative speed bias over NE America

Feature background:

A negative wind speed bias observed at low level over the Eastern USA and Canada during the winter months. AR3 highlighted observations over land with a 'high' height bias relative to the level of best-fit. This was linked to a characteristic of the NESDIS height assignment strategy which assigns low level winds to cloud base over sea, but not over land. The presence of the bias in NH winter was thought to be related to the increase in wind speed and wind shear due to the position of the jet stream.

Update:

The monitoring statistics show that this feature is still present in the IR and visible data from GOES-13. The bias is largest in the IR channel and is observed against both Met Office and ECMWF background fields, though is slightly more marked for the Met Office forecasts. For winter 2012/13 the bias is much more extensive than previous years and is not just confined to over land, but instead spreads out in to the North Atlantic peaking in spatial extent during January 2013 (Figure 1, left). Observed minus best-fit pressure differences are widely in excess of minus 50 hPa, i.e. the AMVs are assigned too high according to the model.

The hourly GOES winds were also being monitored offline at this time allowing us to compare the updated wind product against the operational winds for this feature. Figure 1 shows that the negative speed bias is much reduced in the hourly data, particularly over the North Atlantic, and is now largely confined to land. The exception is an area along the North East US coast where a negative speed bias and 'high' height bias persist against the model. Why is the speed bias reduced over sea for the hourly winds? As well as the winds being extracted more frequently the updated NESDIS product also includes improvements to the height assignment of low level winds. The number of vertical levels from the GFS forecast has been increased and when an inversion is detected over sea the AMV is now assigned to the base of the inversion. The vector plots in Figure 2 show that the mean low level winds at this time are predominantly from the west or northwest and an inversion is likely to be formed where the cold continental air flows over the warm sea surface. Examination of January 2013 mean UKMO model temperature profiles off the NE coast of the USA (not shown) confirm the presence of a low level temperature inversion with a base

around 925 hPa. Hence the improvements observed in the hourly GOES winds are likely the result of better height assignment under inversion conditions.

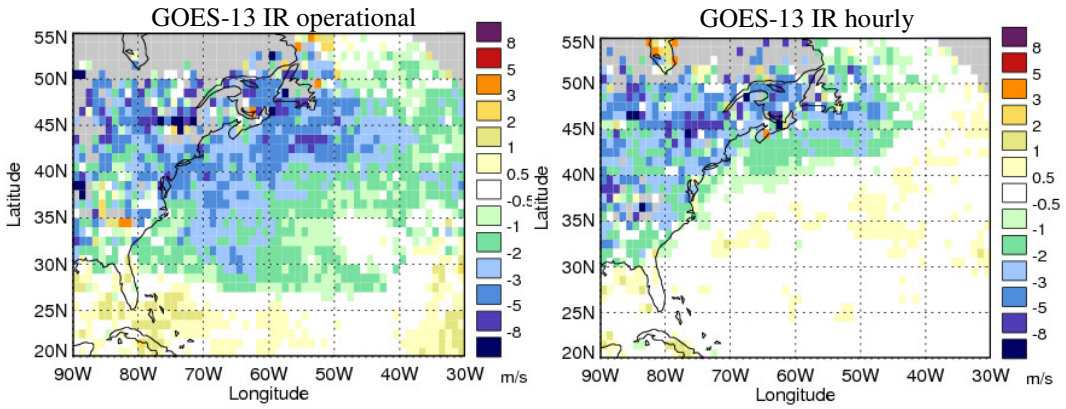


**Figure 1. Map of O-B speed bias for GOES-13 IR AMVs during January 2013: operational data (left) and hourly data (right). Observations filtered for QI2 > 80 and observed pressure below 700 hPa.**

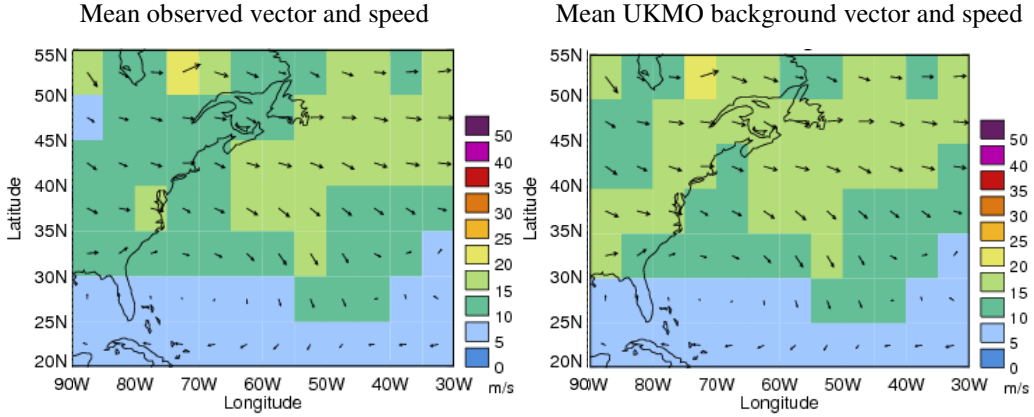


**Figure 2. Mean wind vectors (arrows) and wind speed (colour) for January 2013: GOES-13 hourly IR AMVs (left) and collocated UKMO model background winds (right). Observations filtered for QI2 > 80 and observed pressure below 700 hPa.**

The improved speed bias over sea for the hourly data allows us to focus on the smaller signal near the coast. Figure 3 (left) shows the December 2012 mean speed bias for the GOES-13 IR hourly winds. As seen in the previous example, the negative speed bias over the Atlantic is limited to a narrow region along the east coast. Further north it is noticeable that the bias pattern appears to curve away from the coast near Newfoundland and then curve back northwards at around 40°W. Figure 4 shows the mean analysed foundation sea surface temperature (SST) from the Met Office OSTIA (Operational Sea Surface Temperature and Sea Ice Analysis) system. It is striking that the curve in the bias pattern near Newfoundland appears to match the location of the SST front associated with the Gulf Stream e.g. the tongue of warmer water along 40°W, 45-50°N. It may be that the SST gradient has a direct link

to the bias and a better understanding may be gained from looking at individual cases. The visible winds (Figure 3, right) also show a negative speed bias in similar areas to the IR, but with a less distinct pattern.

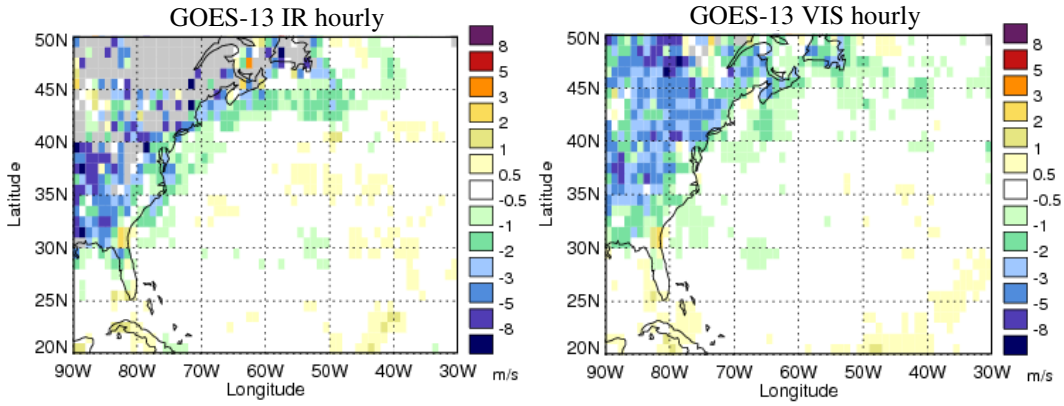


**Figure 3. Map of O-B speed bias for GOES-13 hourly AMVs during December 2012: IR (left) and visible (right). Observations filtered for QI2 > 80 and observed pressure below 700 hPa.**

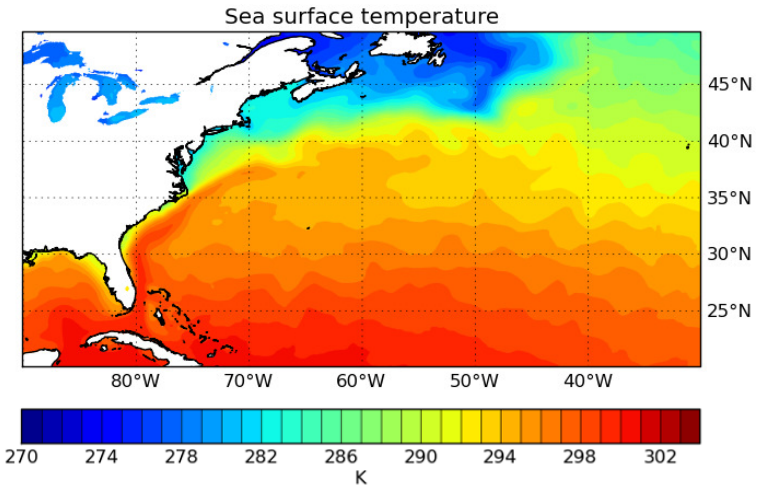


**Figure 4. December 2012 mean SST in the NW Atlantic. Foundation SST taken from the OSTIA reanalysis.**

### *Case study: 30 December 2012, 12z*

A clear speed bias signal can be seen for the 12:00 UTC cycle on 30 December 2012. The Met Office surface pressure chart in Figure 5 shows the general synoptic situation. A surface low (964 Mb) is tracking north-eastwards just off the east coast, driven by an upper trough moving east through the central US. The satellite imagery in Figure 6 shows a cold front clearing out into the Atlantic resulting in an offshore flow with clear skies immediately along the coast. Around 50 km from the coast there is low level cloud formation (cloud top temps around 265k) which forms into streets further offshore. As the day progresses the thicker cloud layer breaks up into more streets. The imagery and model data are consistent with a synoptic-scale cold air

outbreak: the passage of the cold front is dragging a flow of cold, dry air from the continent out over the warm waters of the Atlantic.

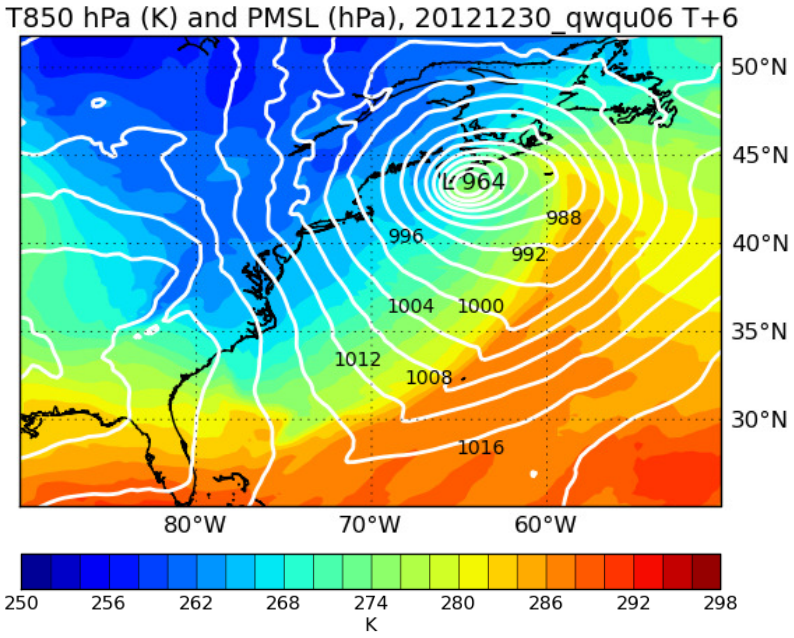


**Figure 5. Temperature at 850 hPa (shaded contours) and MSLP (lines) for the 0600 UTC T+6 forecast valid at 1200 UTC 30 December 2012. Met Office global model forecast.**

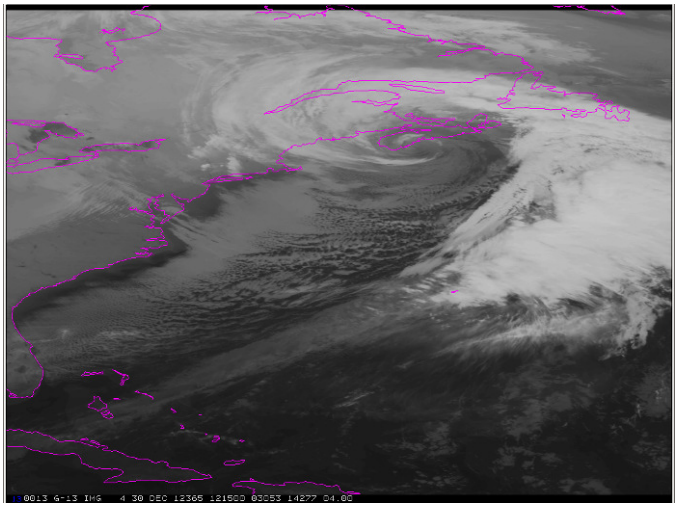

**Figure 6. MCIDAS visualisation of 4 km resolution GOES-13 IR 10.6μ imagery at 1215 UTC, 30 December 2012.**

Figure 7 shows the difference between the AMV and model wind speeds for the hourly IR winds extracted between 0900 UTC and 1500 UTC. The map shows a band of negative wind speed bias just off the coast, particularly around 68°-70°W, 35°-40°N where O-B's are in excess of minus 3 m/s. The bias is mainly constrained to observations extracted closest to the coast tracking the formation of cloud streets, plus a few tracking holes in the cloud layer. AMV assigned pressures (not shown) are

mostly below 850 hPa but model best-fit pressure estimates are not well-constrained for most of the problem winds. The poor fit to the model may be because there is nowhere low enough in the model wind profile to match the slower AMV observations. Most winds have been assigned heights using the cloud base method, but some of the biased winds slightly further away from the coast have been assigned WV intercept heights (Figure 7, right).

A closer inspection of the wind vectors over the main area of interest (Figure 8) shows that the AMVs and model are generally in good directional agreement. The observations located north of 38°N in Figure 8 clearly show the difference in wind speed: AMV speeds around 15-17.5 m/s, model speeds 17.5-20 m/s. AMVs assigned WV intercept heights in Figure 8 correspond to the faster model vectors (e.g. shaded green) around 35°-36°N and show poor agreement in both speed and direction. The WV intercept method is always likely to be unsuccessful in this situation due to the reduced sensitivity of WV channels in the lower troposphere. It is likely these winds have been assigned too high (Figure 9) but these few observations are not responsible for the more widespread speed bias. Figure 9 shows that for winds assigned to cloud base, the negative speed bias is greatest below 900 hPa (lowest levels). Combined with the poorly constrained model best-fit pressure, this suggests that the negative bias is not the result of a height assignment error (as assigning higher up would only lead to a worse fit).

The GOES-13 hourly visible winds in this case are generally very similar and exhibit the same pattern of negative speed bias nearest the coast and poorly constrained best-fit pressure.

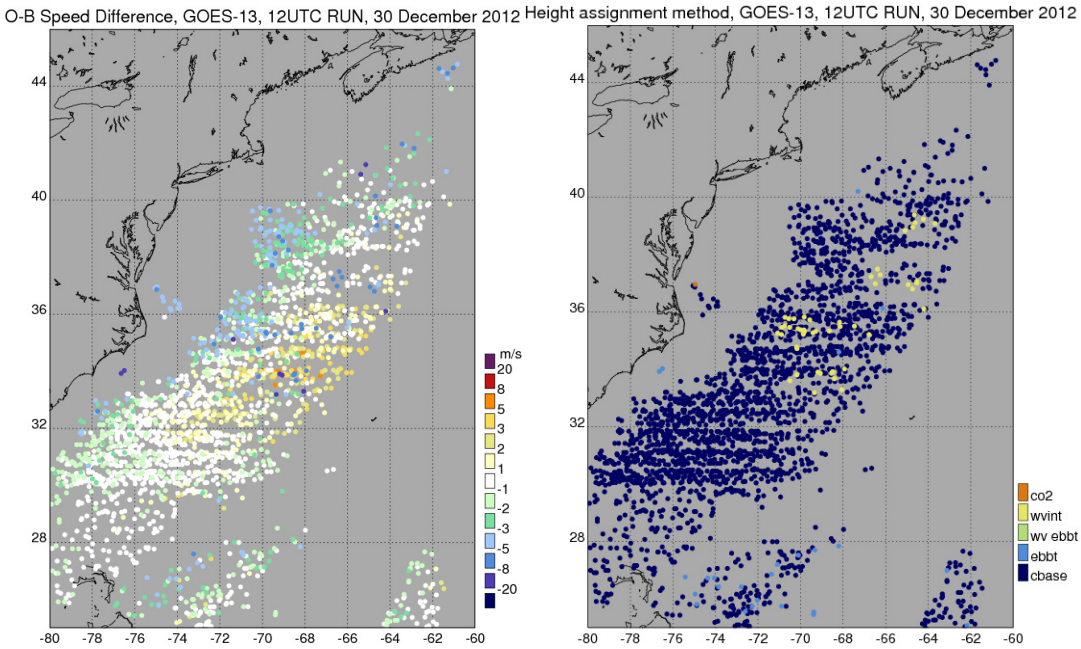


**Figure 7. Map of O-B speed bias (left) and height assignment method (right) for GOES-13 hourly IR AMVs valid at 12:00 UTC 30 December 2012. Observations filtered for QI2 > 80 and observed pressure below 700 hPa.**

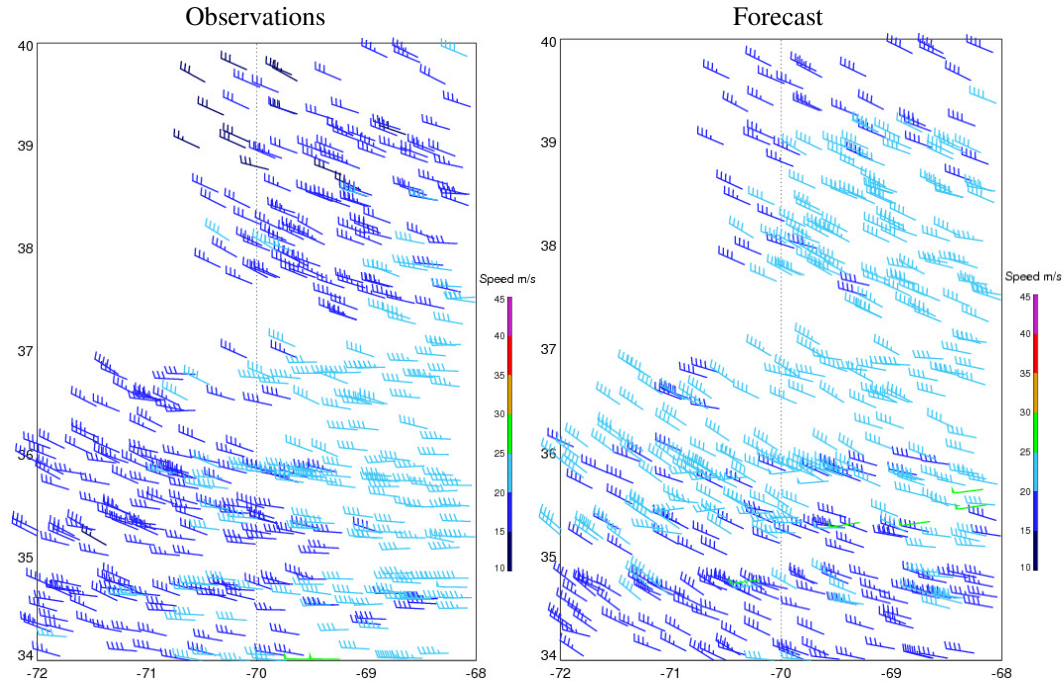


**Figure 8. AMV wind vectors (left) compared with collocated model winds (right). IR AMVs valid at 12:00 UTC 30 December 2012. Observations filtered for QI2 > 80 and observed pressure below 700 hPa.**

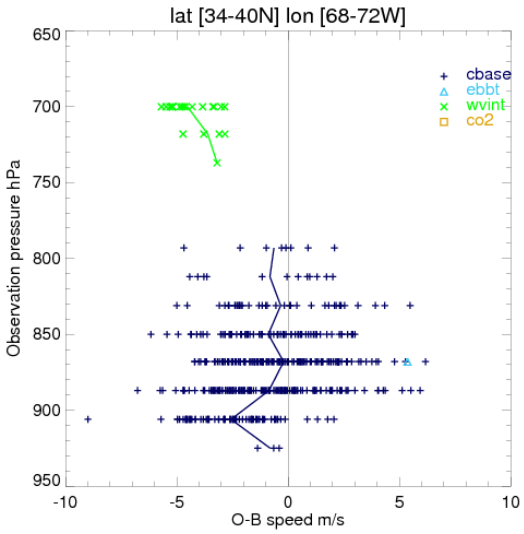


**Figure 9. Scatter plot of speed bias versus pressure for the AMVs plotted in Figure 8. Lines show the mean bias for each pressure level.**

To diagnose the cause of the bias we also need to consider the quality of the NWP model background. Figure 10 (left) shows the Met Office short range (T+6) forecast wind speed and vectors at the 850 hPa pressure level. The AMV speed bias is associated with the area of moderate winds (green shades) flowing offshore, between Washington and Rhode Island. Could the model winds be too strong in this case? Figure 10 (right) shows the difference between the Met Office T+6 and ECMWF T+12 short range forecasts valid at 1200 UTC. Note there are clearly some large differences over the Atlantic due to the exact position of the low pressure system and associated fronts. In the region of moderate winds mentioned above it can be seen that the flow is stronger in the Met Office forecast for the first couple of hundred km offshore. In particular note the area shaded red located 68-70°W, 38-40°N where the Met Office model winds are faster by about 2 m/s: this coincides well with the AMV speed bias of similar magnitude seen in Figure 7. Overall there is enough evidence here to suggest that the Met Office model may be overestimating the strength of the low level winds and contributing at least in some part to the observed bias versus the AMVs.

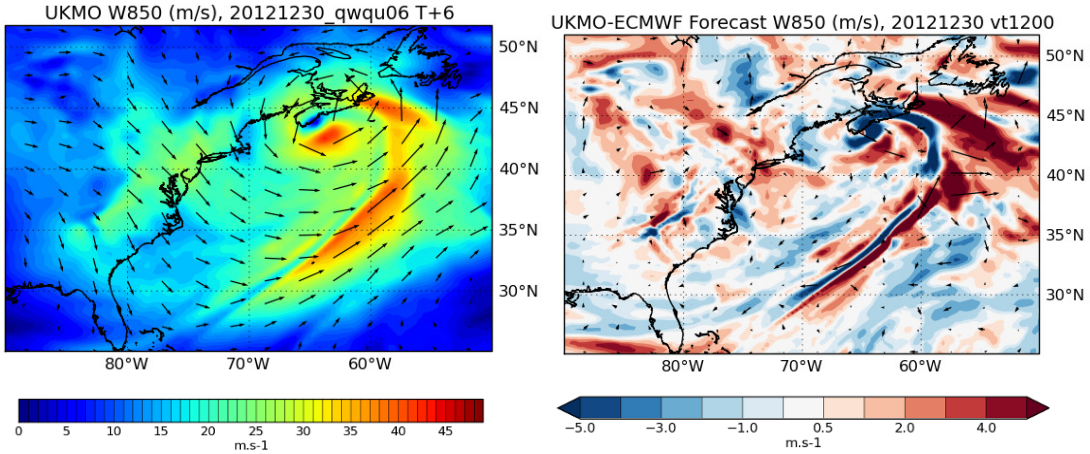


**Figure 10. Met Office T+6 forecast winds at 850 hPa (left) valid at 12:00 UTC 30 December 2012. The wind arrows have been thinned to 1 in 8 for ease of display. Also plotted is the difference in forecast winds (right) between the Met Office (T+6) and ECMWF (T+12) valid at the same time.**

Another possible cause of the bias can be seen by looking at the O-B speed bias overlain on the IR imagery as demonstrated by Figure 11. In the image, negative speed biases are shaded from light blue to dark blue and positive speed biases from green to yellow. It is noticeable that the AMVs with the largest negative speed bias tend to be located near to where the low level stratocumulus is breaking up. This suggests that the AMV tracking algorithm may not be handling this kind of situation well and/or that such clouds do not make good tracers. The reason for the cloud deck breaking up in that location is likely related to the cold air encountering the increasingly warm SST's of the Gulf Stream. The vertical transfer of heat and moisture from the ocean surface will promote over-turning and mixing of the lower layers helping to break up the cloud. This would explain why the monthly mean speed bias pattern in Figure 3 appears to coincide with the SST gradients. Norris and Iacobellis (2005) found that along the N. Pacific SST front, the breakup of cloud occurs due to the decoupling of the marine boundary layer as it is advected south over warmer water.

Overall, the evidence here suggests that the bias observed during cold air outbreaks is linked to the accuracy of the short-range NWP forecast and difficulties tracking the breakup of cloud along the SST front. The response of low level clouds to the Gulf Stream has recently been investigated by Liu et al. (2014) using a combination of CALIPSO and reanalysis data. They found that the sharp SST front exerts a strong influence on low level clouds. In particular the low level cloud tops over the warm water were found to be on average 0.5 km higher than over cold water. Under cold northerlies strong instability leads to a well-mixed boundary layer and a deepening of low level clouds across the SST front.

A similar case to the one described above can be seen on the 22 December 2012. The synoptic situation is very similar with a deep low pressure tracking northeast and trailing cold front leading to another cold air outbreak. The cloud formation along the coast is strikingly similar (Figure 12) and again the AMVs tracking the offshore cloud streets exhibit a negative speed bias near the coast.

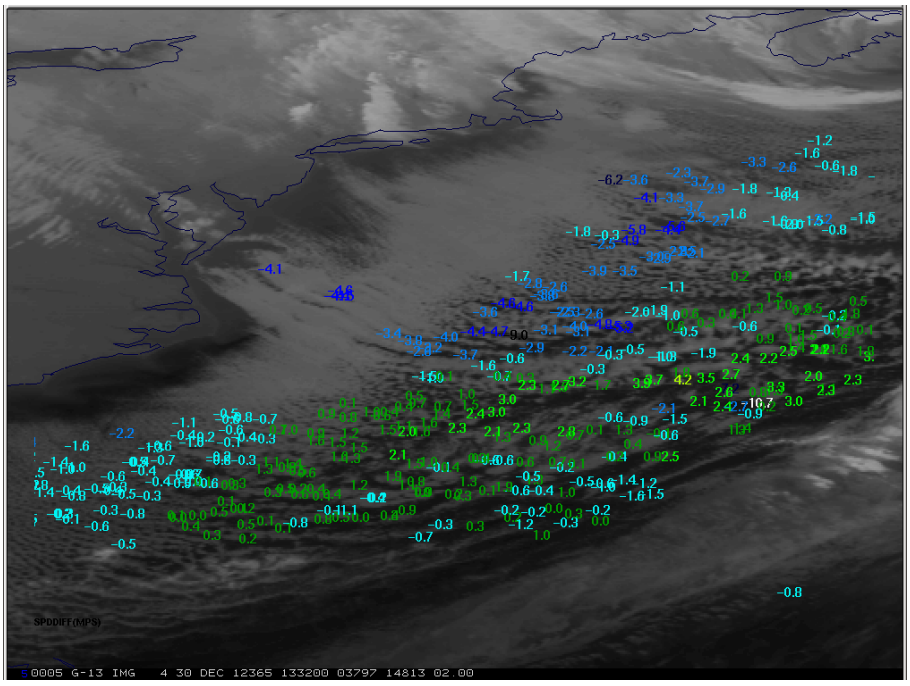


**Figure 11. O-B speed bias values overlain on the IR image from 13:30 UTC. IR AMVs extracted between 13:00-14:00 UTC and filtered for QI2 > 80 and observed pressure below 700 hPa.**

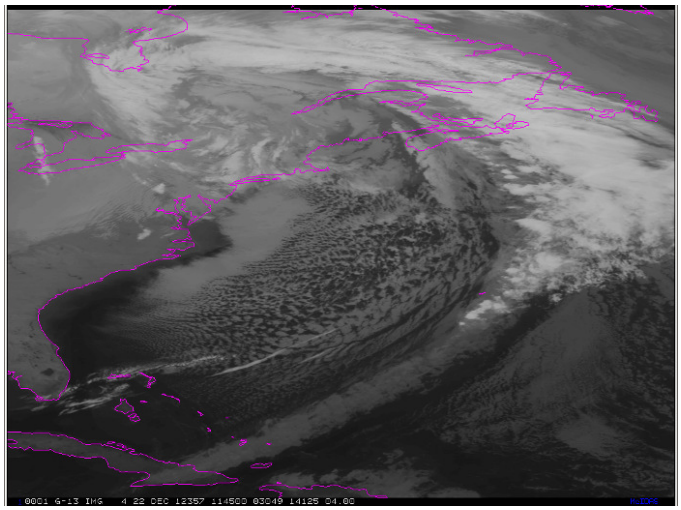

**Figure 12. MCIDAS visualisation of 4 km resolution GOES-13 IR 10.6 imagery at 1215 UTC, 30 December 2012.**

### Feature 2.6. MSG positive bias over North Africa

Feature background:

A large positive wind speed bias is observed in the MSG IR and visible channels over North Africa and the Arabian Peninsula during winter. Although mainly over land, the bias does extend over the Atlantic to the west of Africa in January/February and also moves northwards into the Mediterranean by May. AR4 linked the bias to large height assignment errors when tracking cirrus clouds, leading to very fast winds being assigned around 500 hPa too low. The feature closely matches the location of the sub-tropical jet stream.

Update:

The general characteristics of this feature have remained largely unchanged with the switch from Meteosat-9 to Meteosat-10 (January 2013) and the implementation of the CCC scheme (September 2012). The bias is largest in magnitude for the IR winds and is more marked in the high resolution visible data compared to the visible at 0.8μ. Comparing a parallel period of Meteosat-9 and Meteosat-10 data from January 2013 confirms no impact from the change of satellite. However the subsequent winter months in 2013 appear to show a slight improvement for the visible channel winds compared with the same period in 2012. Figure 13 and Figure 14 show an example of this for the visible 0.8μ winds. In March 2013 the positive speed bias is less widespread and there are fewer winds extracted in the problem area between15-30°N over the Sahara. Levels of mean vector difference are also reduced in common areas observed in both years (not shown). These changes could be just due to seasonal/inter-annual variations in cloud distributions. However as this trend is also present in February and April it also could be that this improvement is due to changes introduced with the CCC scheme. As visible channel radiances cannot be used to directly calculate the cloud top height the IR channel brightness temperatures are used instead. Under the old EUMETSAT height assignment scheme the coldest IR pixels in the target box were used to set the cloud top and this introduces an error when these pixels do not match the feature being tracked in the visible. This is particularly significant in multi-layer cloud situations. With the CCC scheme only the IR radiances of the (brightest) pixels that are driving the tracking in the visible channel are selected. The improved pixel selection is perhaps why we are seeing some improvement in the visible channels for this bias.

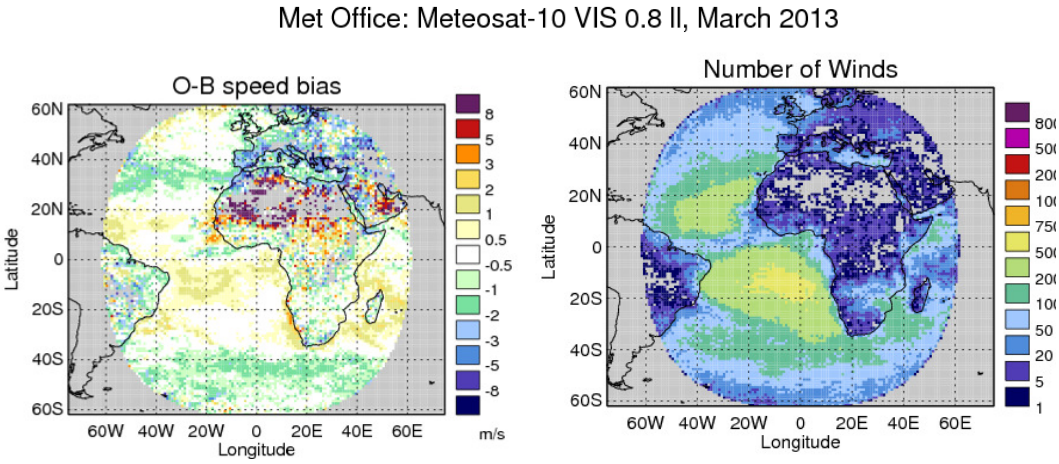


**Figure 13. Map of O-B speed bias (left) and the distribution of winds (right) for Meteosat-10 visible 0.8 AMVs during March 2013. Observations filtered for QI2 > 80 and observed pressure below 700 hPa.**

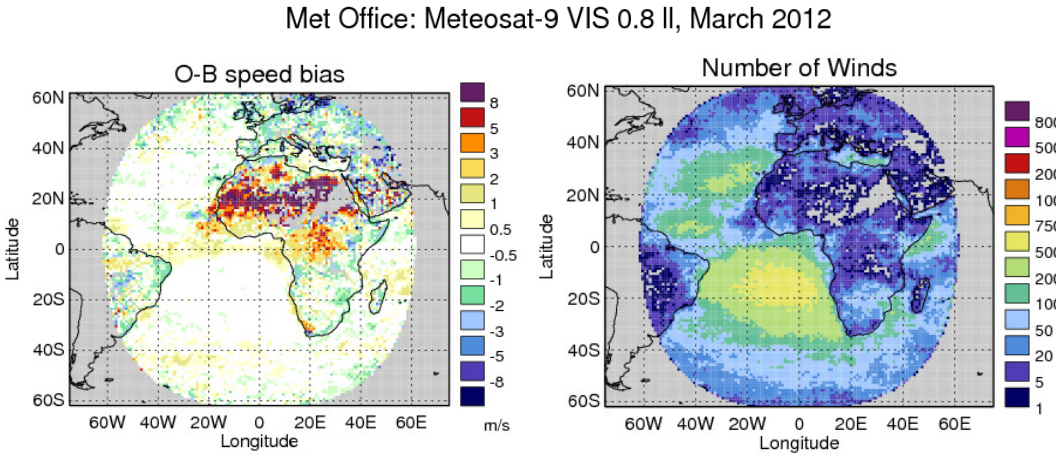


**Figure 14. As Figure 13 but for Metoesat-9 winds during March 2012.**

## Feature 2.7. Spuriously fast Meteosat and MTSAT winds

Feature background:

Both Meteosat-7 and MTSAT show regions with very fast wind vectors assigned at low levels. For Meteosat-7, AR4 identified features associated with 1) the summer monsoon period and 2) near India during northern hemisphere winter. In both cases the bias was linked to large height assignment errors in areas of high vertical wind shear, namely the Tropical Easterly Jet (leading to a poor representation of the monsoon winds) and the sub-tropical jet (peaking in winter months).

MTSAT IR AMVs have shown large positive speed biases in several areas: a) off the NW coast of Australia, b) in the South China Sea and c) South Pacific Convergence Zone.

Update:

The Meteosat-7 biases generally remain as described in previous analysis reports and are not discussed further here.

The O-B speed bias statistics for MTSAT-2 show a large difference between the IR and visible channels. Whereas the visible data shows good agreement with collocated model wind speeds, the IR exhibits significant biases against both Met Office and ECMWF forecasts. Figure 15 shows an example of the positive bias seen around the South China Sea for the IR winds versus the ECMWF background. It is not clear why there is such a marked difference between the two channels but differences include:

- Image resolution: IR 4-km, visible 1-km at sub-satellite point
- Target box size: IR 16x16 (for 15-min winds) or 24x24 (30/60-min winds), visible 40x40 pixels
- Visible AMVs daytime only

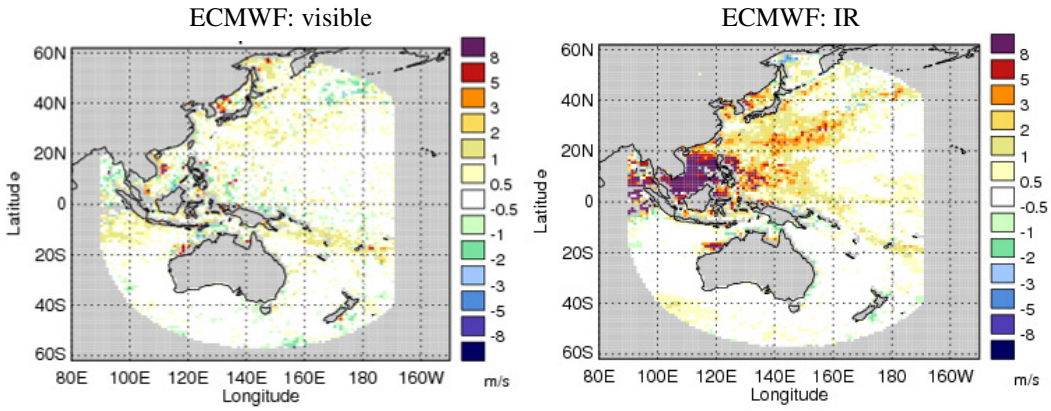


**Figure 15. Maps of O-B speed for MTSAT AMVs during August 2013 versus the ECMWF model background: visible winds (left) and IR (right). Observations filtered for QI2 > 80 and observed pressure below 700 hPa.**

Another curious feature of the MTSAT IR winds at low level can be observed in the 2-D histograms of observed versus background wind speed (Figure 16). In the northern hemisphere extra-tropics and the tropics there is an unusual change in the wind distribution at observed speeds of 15 m/s. There appears to be a high number of AMVs assigned speeds up to 15 m/s for which the model estimates are much slower.

Figure 17 shows the RMS vector difference versus the Met Office model as a function of wind speed. There is a steep rise in RMSVD as the AMV speed approaches 15 m/s (circled), after which there is a temporary drop-off. The histogram of the number of winds (Figure 17, right) also shows a 'bulge' in the distribution around 11-15 m/s when the data is binned by observed speed (red line), but not when binned by model speed (blue). Observations in the southern hemisphere extra-tropics are unaffected by this feature.

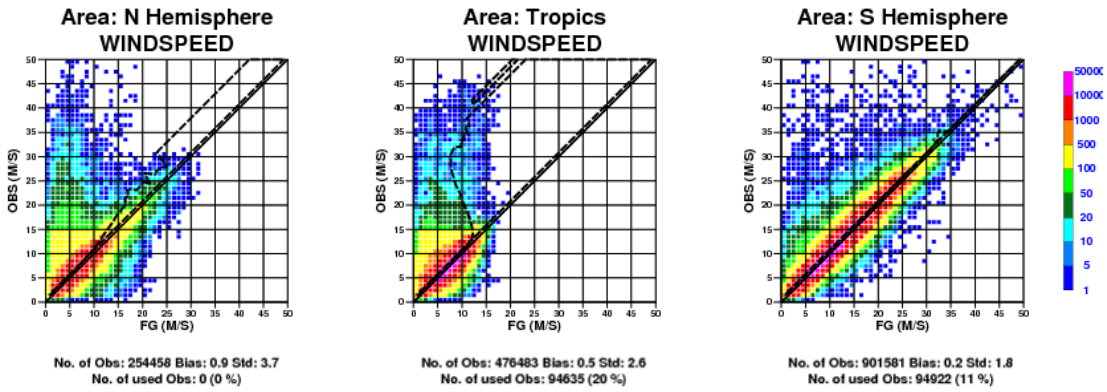


**Figure 16. Two dimensional histograms of observed wind speed versus ECMWF model wind speed for MTSAT-2 IR AMVs in August 2013. The colour shading of each box represents the number of observations. Observations filtered for QI2 > 80 and observed pressure below 700 hPa.**

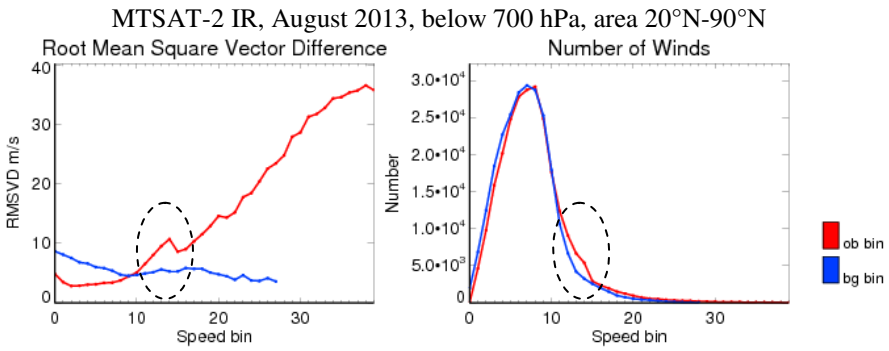


**Figure 17. MTSAT-2 IR winds for August 2013: RMS vector difference (left) and number of winds (right) as a function of observed/background wind speed. Observations filtered for QI2 > 80, observed pressure below 700 hPa and latitude greater than 20°N. The feature of interest has been circled in black.**

In July 2013 a chain of positive speed bias can be seen stretching out in to the Pacific, south of Japan (Figure 18). Again this feature is not present in the visible channel data. Examination of O-B speed bias as a function of latitude and time shows a strong signal around 30°N for 5-7 July 2013. Figure 19 compares MTSAT-2 IR and collocated model wind vectors for a case at 18:00 UTC on 5 July. There is a very marked disagreement in both wind speed and direction for the line of winds nearest the top of the image: observations widely in excess of 20 m/s from the E or

NE, model vectors generally less then 10 m/s from the S or SW. In the worst case, for vectors near 24°N 128°E, the AMV speeds are 41 m/s whilst the model estimates are just 7 m/s.

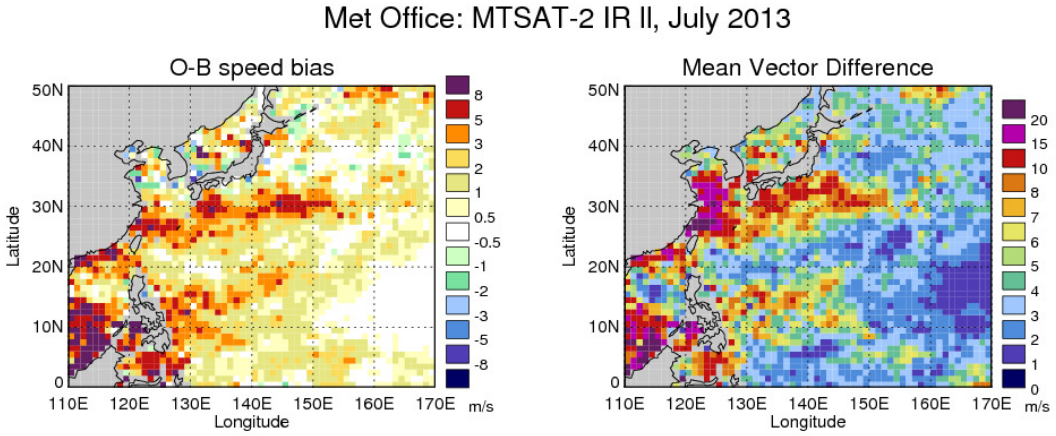


**Figure 18. Maps of O-B speed (left) and MVD (right) for MTSAT IR AMVs during July 2013 versus the Met Office model background. Observations filtered for QI2 > 80 and observed pressure below 700 hPa.**

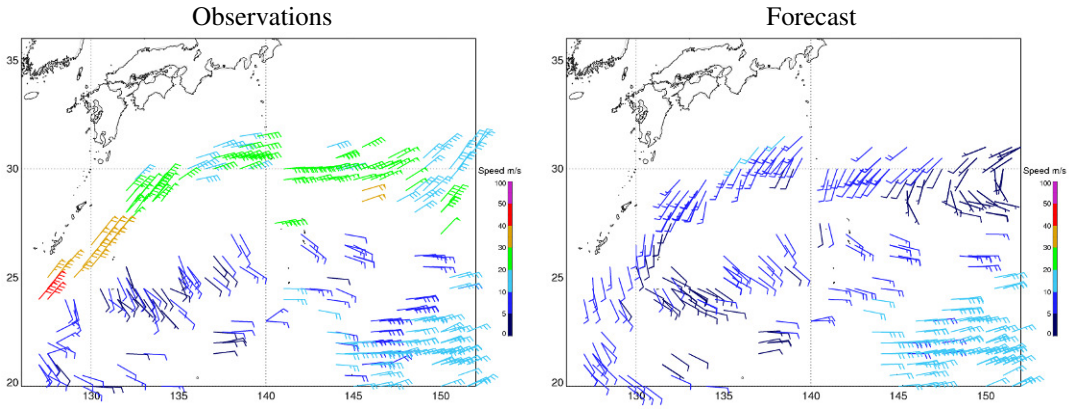


**Figure 19. AMV wind vectors (left) compared with collocated model winds (right). MTSAT-2 IR AMVs valid at 18:00 UTC 05 July 2013. Observations filtered for QI2 > 80 and assigned pressure below 700 hPa.**

The large O-B difference in both speed and direction suggests a large error in height assignment. This is confirmed by comparing the assigned pressures with model best-fit pressure estimates (Figure 20). AMVs along the line of very fast winds have been assigned heights in the range 850-880 hPa whilst model estimates are fairly well-constrained to 140-200 hPa, giving a pressure difference of over 700 hPa. Imagery shows this gross height assignment error is from tracking cirrus cloud.

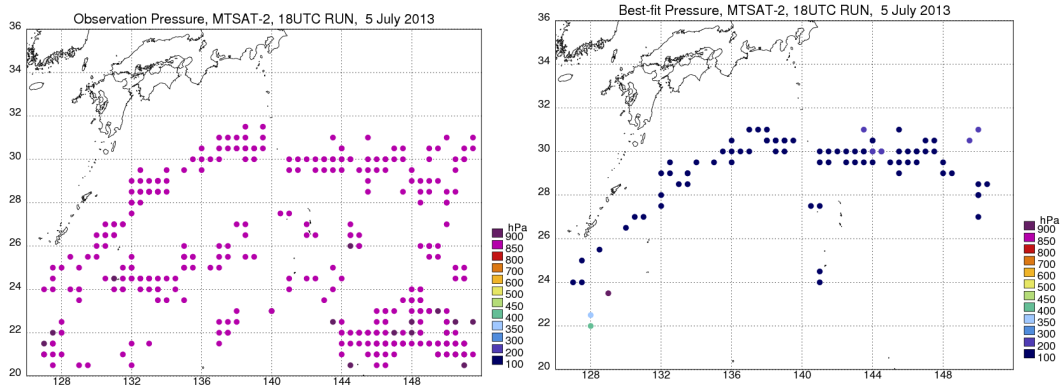


**Figure 20. Assigned AMV pressure (left) and model best-fit pressure (right) for MTSAT-2 IR winds valid at 18:00 UTC 5 July 2013. Observations filtered for QI2 > 80 and assigned pressure below 700 hPa.**

An "A-train" overpass at around 17:00 UTC provides further validation of the feature being tracked by the AMVs. MODIS cloud top temperatures from Aqua (Figure 21) show that the AMVs are tracking the southerly edge of a cold, high cloud top (blue shading) with a fringe of warm low level cloud (red shading). The corresponding image of MODIS cloud top pressure (not shown) has retrieved values for the cold-cloud feature above 200 hPa. The MODIS result is backed up the CALIPSO vertical profile in Figure 22 which has a cloud top at around 15-16 km (approx. 110-130 hPa) for the edge of the high cloud at 29°N.

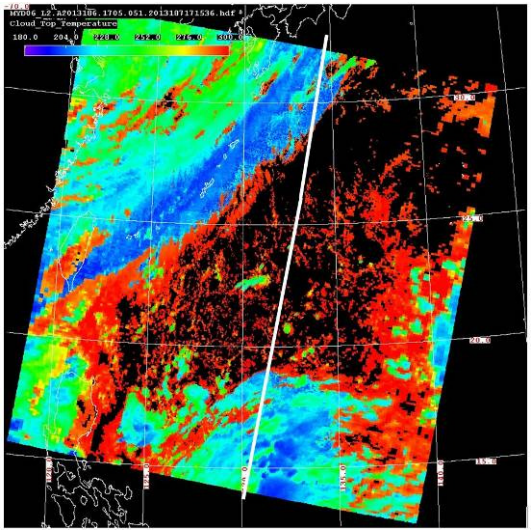

**Figure 21. MODIS Aqua cloud top temperature at 17:05 UTC 5 July 2013. Approximate ground track of CALIPSO overpass shown in white. Image from the NASA Atmosphere Archive and Distribution System (LAADS).**

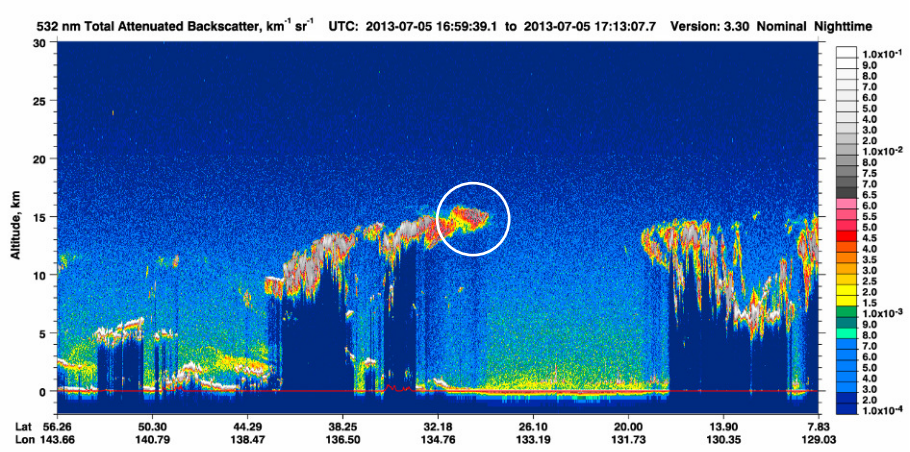


**Figure 22. CALIPSO 532 nm Total (Parallel + Perpendicular) attenuated backscatter (/km/sr). The cloud edge of interest has been circled.**

For the subsequent 00 UTC cycle on the 6 July, the IR AMVs have very similar bias characteristics as described above: a line of faster winds from the E/NE continuing to track the high cirrus cloud (Figure 23, left). As 00 UTC is a daytime cycle for MTSAT we can now also compare with the visible AMVs. Figure 23 (right) shows there are no visible channel AMVs tracking the cirrus embedded in the upper level easterly flow and as a result the visible AMVs extracted in this region show good agreement with collocated model vectors. This may give some indication as to why the monthly mean O-B maps as in Figure 15 look so much better for the visible AMVs.

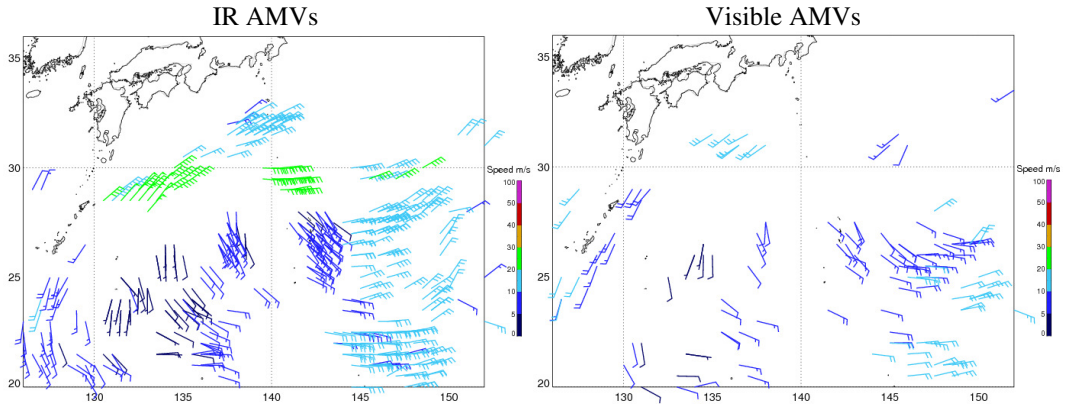


**Figure 23. MTSAT-2 IR (left) and visible (right) AMVs valid at 00:00 UTC 06 July 2013. Observations filtered for QI2 > 80 and assigned pressure below 700 hPa.**

### Feature 5.2. MSG negative bias during Somali Jet

Feature background:

A marked negative wind speed bias observed near the north east tip of Somalia during July and August. The bias is very prominent in the visible 0.8μ and high resolution visible channels versus both Met Office and ECMWF models, but less noticeable in the IR winds. In AR5 the bias was shown to be associated with the peak in strength of the low level Somali Jet and investigation revealed O-B differences in excess of minus 20 m/s. The cause of the bias for the visible data was linked to instances of height assignment error, the influence of a small mountainous island within a very strong wind regime and the enhanced spatial resolution of the visible imagery versus the IR.

Update:

When compared with 2012 the monitoring plots from July and August 2013 show that the negative speed bias is now also very prominent in the IR winds. The magnitude of the bias in the visible 0.8μ channel looks relatively unchanged, but in the high resolution visible the negative bias appears worse than ever (Figure 24). What is the likely cause of these changes? Prior to the CCC scheme being implemented in September 2012 a parallel stream of test data was made available by EUMETSAT. Comparing the July 2012 O-B maps of the operational (at that time) and CCC data reveals little or no impact on the Somali Jet speed bias from the new height assignment scheme in either the IR or visible channels (not shown). There is no way to tell if there has been any impact from the switch to Meteosat-10. The most probable reason for the apparent worsening of the bias is that the Somali Jet was stronger in 2013 than in the previous year. As shown in Figure 25 the 26 m/s contour level covers a much wider region in 2013 and the peak wind speed within the jet is over 1 m/s higher than in 2012.

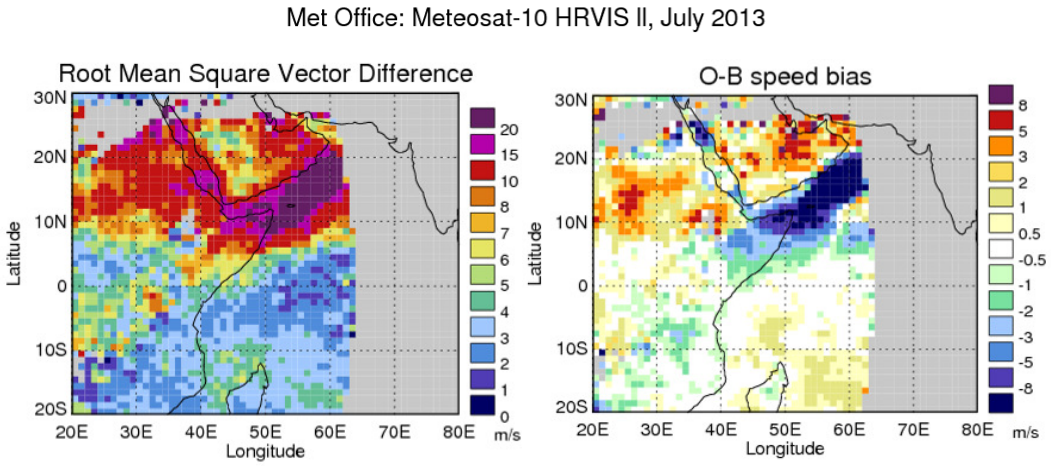


**Figure 24. Map of RMS vector difference (left) and O-B speed bias (right) for Meteosat-10 high resolution visible AMVs during July 2013. Observations filtered for QI2 > 80 and observed pressure below 700 hPa.**

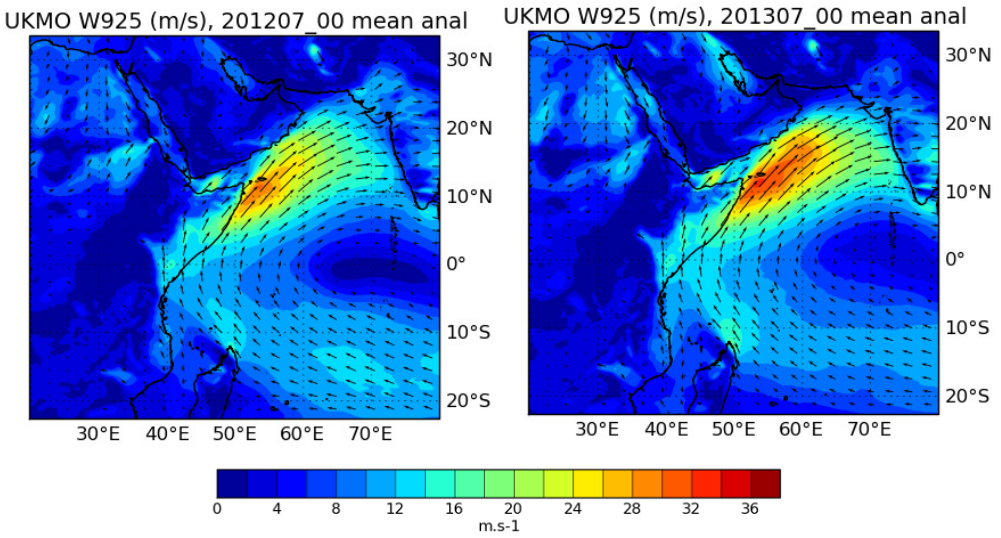


**Figure 25. Mean Met Office analysis wind speed (contours) and wind vector (arrows) at 925 hPa for July 2012 (left) and July 2013 (right).**

## Feature 6.1. Bias in tropical East Atlantic

New feature:

An unusual bias pattern can be observed in the tropical East Atlantic near the Cape Verde islands during May and June 2013 (Figure 26). The feature is characterised by an area of positive bias located around 20°W, 10°N which is bounded to the north, south and west by a negative speed bias. It is prominent in both the IR and visible 0.8μ data but is less marked in the high resolution visible where only the northern branch of the negative speed bias is present.

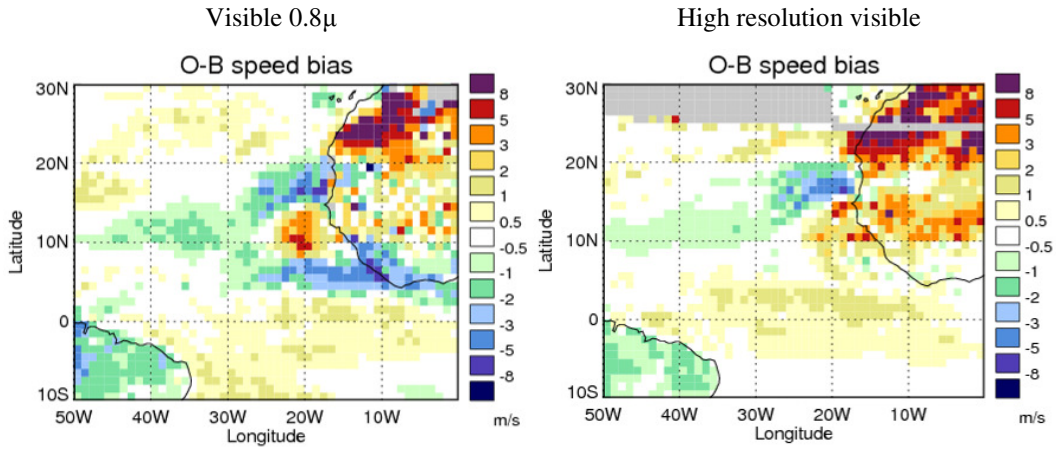


**Figure 26. O-B speed bias for Meteosat-10 visible 0.8μ (left) and high resolution visible (right) AMVs during May 2013. Observations filtered for QI2 > 80 and observed pressure below 700 hPa. The map for the IR winds is very similar to the visible 0.8 image.**

Hovmoeller plots (not shown) comparing O-B's as a function of latitude and time suggest that the strongest positive/negative speed bias signals in the Eastern Atlantic occur rather separately. The positive speed bias around 10°N is most prominent between 6-9 May inclusive, the negative speed bias around 7°N between 22-25 May and the negative bias around 17°N between 25-31 May.

If we focus on the positive speed bias, Figure 27 shows that the area of positive bias moves progressively further north on each successive day between May 6 and May 9. O-B speed biases for the visible 0.8μ AMVs are in excess of +8 m/s. The plots for the 7-8 May also show a more widespread negative speed bias west of 32°W, consistent with the monthly plots above.

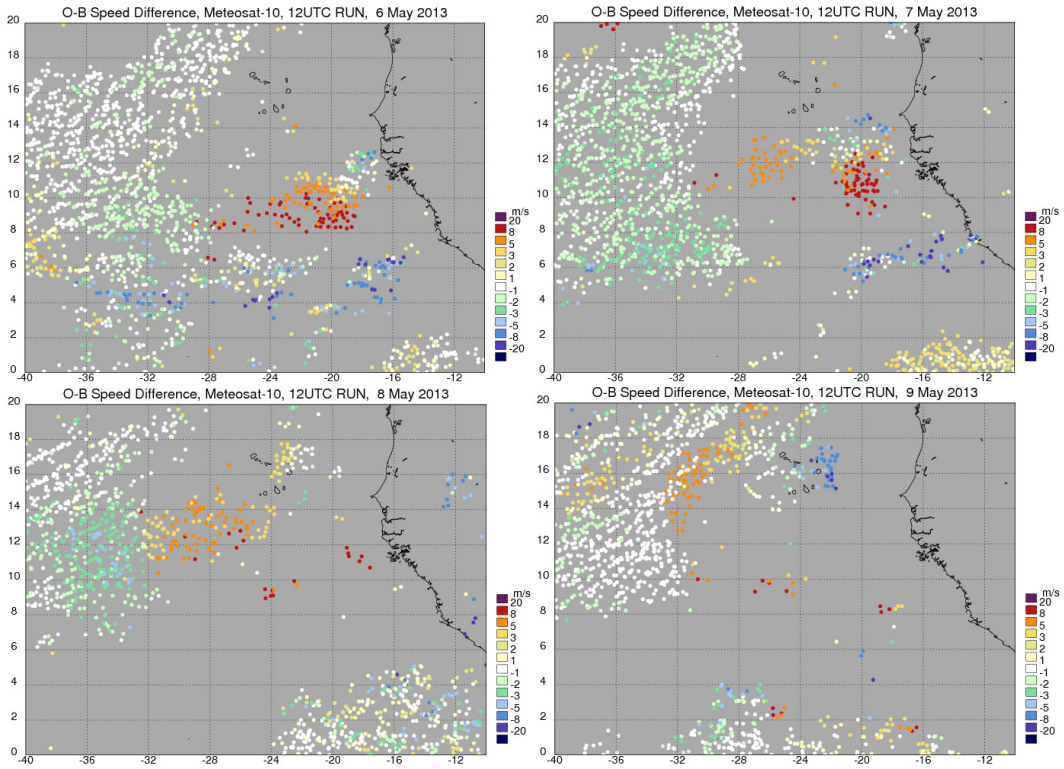


**Figure 27. Maps of O-B speed for Meteosat-10 visible 0.8μ AMVs valid at 12:00 UTC on 6 (top left), 7 (top right), 8 (bottom left), 9 (bottom right) May 2013. Observations filtered for QI2 > 80.**

Figure 28 compares Meteosat-10 visible AMVs extracted at 10:30 UTC on 7 May with collocated model background wind vectors. The (positive) biased observations are associated with two areas.

1) AMVs located to the south of the Cape Verde Islands are tracking fairly thin clouds with assigned vectors of 10-12.5 m/s from the ESE and assigned heights of 960 hPa (Figure 29, left). The collocated model winds in this case are slower by around 5 m/s and from the NE giving poor directional agreement. Best-fit pressure estimates are not widely constrained for this group of vectors but those that are range from 570-620 hPa.
2) Off the African coast there is an arc of brighter cloud on the visible image which is being tracked moving from the E or SE at around 17.5 m/s. AMVs in this case have again been assigned to 960 hPa. The model background winds are around 7.5-12.5 m/s from the NE, and to the south of this feature the model begins to show cyclonic circulation such that AMV and model differ by 180 degrees. Model best-fit pressure estimates are fairly well-constrained to 580-640 hPa away from the southern portion of the cloud. It is noticeable that the one vector located at 10.3°N 17.7°W which has been assigned higher at 739 hPa, agrees much better with the model.

The evidence from the model suggests that the problem AMVs and are in fact tracking mid level clouds and have been assigned too low by 300-400 hPa. For the AMVs to the south of Cape Verde this is probably because the clouds are very thin and so the IR window height assignment will contain contributions from below the cloud. For the arc of brighter cloud the situation is less clear. The Met Office MSG cloud top height product (Figure 29, right) shows a large spread in retrieved pixel pressures for this feature. The histogram in Figure 30 shows some retrieved pixel heights above 200 hPa, a fair amount of mid level cloud, but also low cloud below 900 hPa.

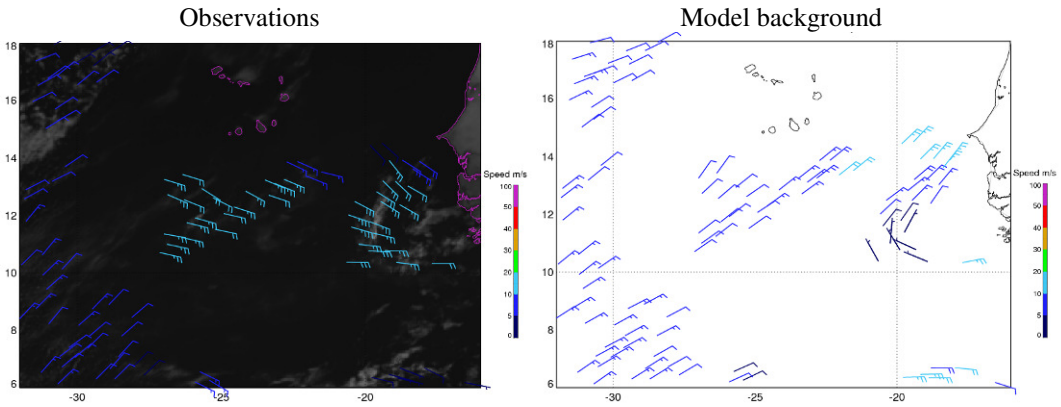


**Figure 28. AMV wind vectors (left) compared with collocated model winds (right). Visible 0.8µ AMVs extracted at 10:30 UTC 07 May 2013 and overlain on an MSG visible image from 10:27 UTC. Observations filtered for QI2 > 80.**

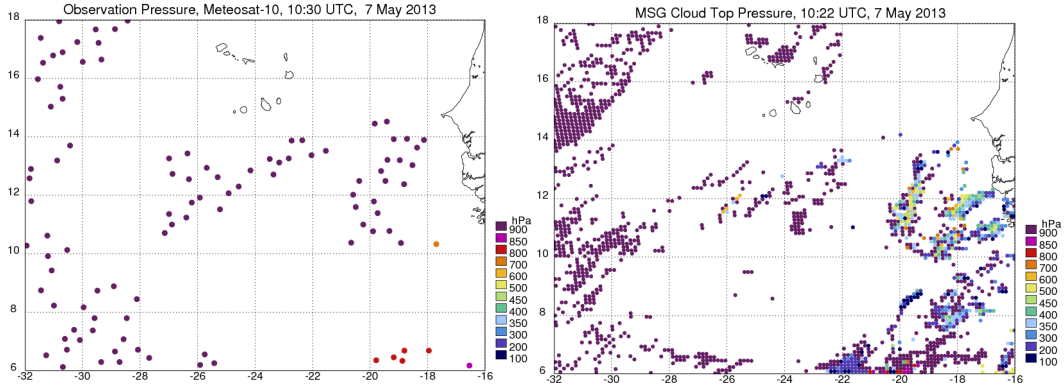


**Figure 29. Left: Map of AMV assigned pressure (left) for Meteosat-10 visible 0.8µ AMVs at 10:30 UTC 07 May 2013. Observations filtered for QI2 > 80. Right: Met Office MSG cloud top pressure product for 10:22 UTC.**

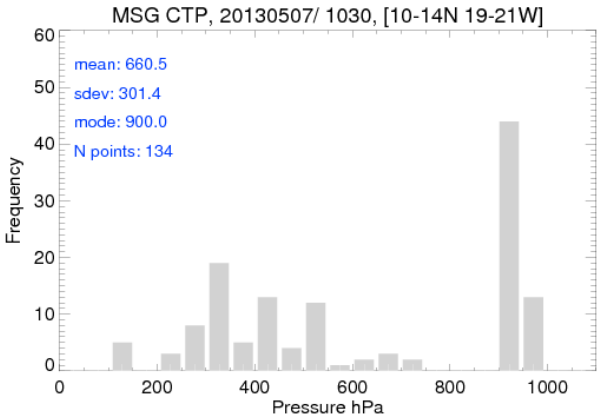


**Figure 30. Histogram of MSG cloud top pressure for the arc of cloud located 10-14°N, 19-21°W.**

A later overpass by Aqua at 15:05 UTC also captured the arc of cloud as it progressed westwards. The MODIS cloud top pressure estimates around 600-700 hPa (green shading) are consistent with the theory that the AMVs have been assigned too low. Note the vertical stripe in the cloud top height and RGB image due to sun glint (solar reflectance off the ocean surface) which can also be observed in the MSG visible images at this time.

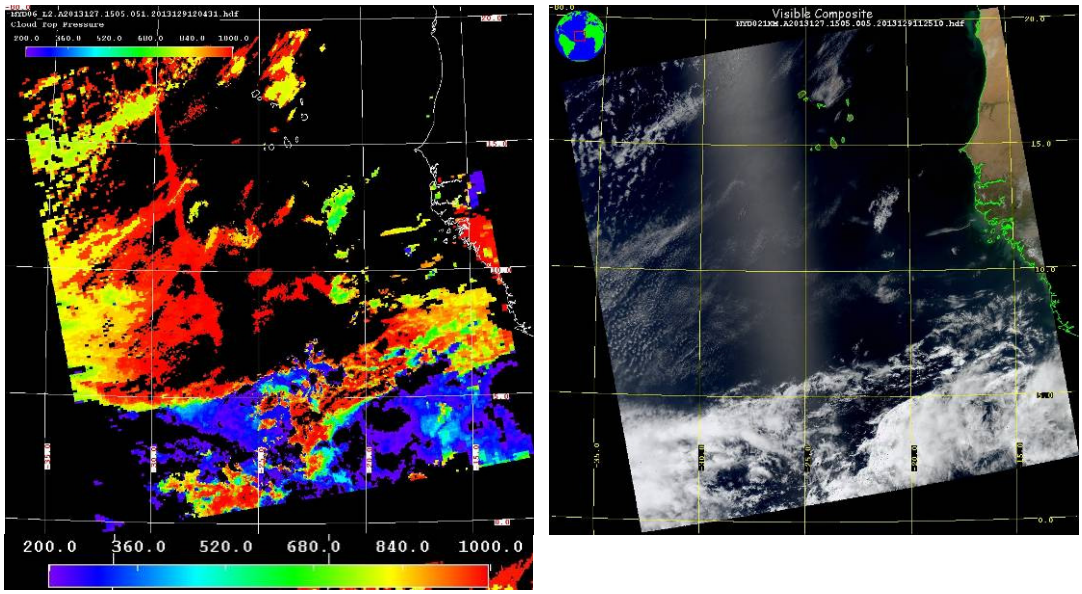


**Figure 31. Aqua MODIS cloud top pressure (left) and RGB image (right) at 15:05 UTC 7 May 2013. Images taken from the NASA Atmosphere Archive and Distribution System (LAADS).**

## Feature 6.2. MTSAT and FY-2E bias during NE winter monsoon

New feature:

The most prominent feature for low level IR winds from FY-2E is a marked negative speed bias in the northern hemisphere during the winter months from November to March. This is clearly evident in 2-D histograms of observation versus background speed for both Met Office and ECMWF models. An example for January 2013 is shown in Figure 32 where the mean O-B speed has reached minus 2.5 m/s. The other latitude bands show relatively little speed bias throughout the year.

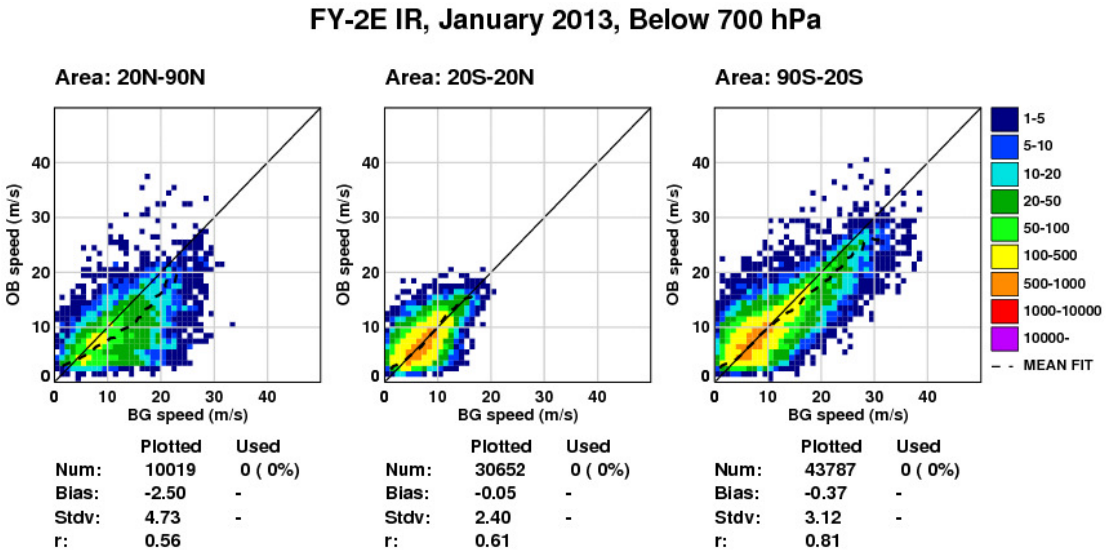


**Figure 32. Two dimensional histograms of observed wind speed versus background wind speed for FY-2E IR AMVs in January 2013. The colour shading of each box represents the number of observations. Observations filtered for QI2 > 80 and observed pressure below 700 hPa.**

The FY-2E low level map plots show that the negative speed bias is localised to a region near Korea and Japan (Figure 33, left). It is also noticeable that the low level IR winds from MTSAT-2 show a negative speed bias in the same region, but the magnitude of the bias is much less (Figure 33, right). Comparing the mean observed and collocated model wind vectors (Figure 34) for FY-2E shows that the bias is the result of the observations underestimating the strength of winds flowing off the Asian continent. The vector plots for MSTAT-2 (not shown) display something similar but restricted to coastal areas.

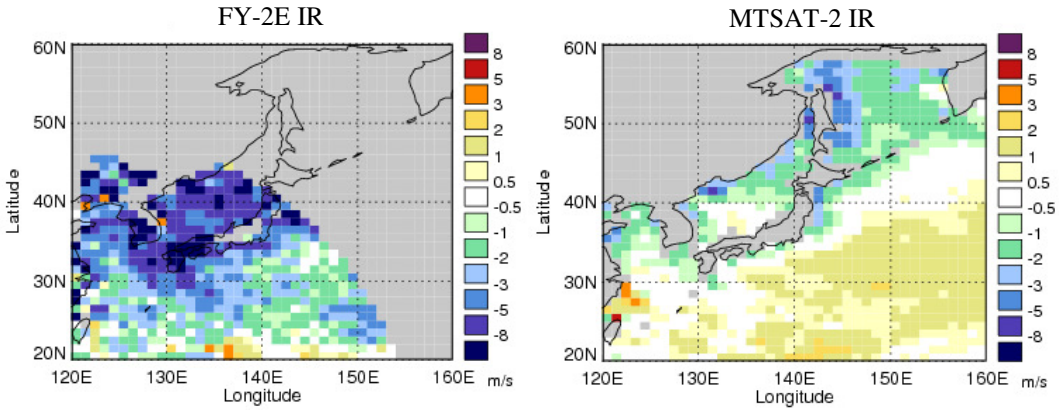


**Figure 33. Map of O-B speed bias for FY-2E (left) and MTSAT-2 (right) IR AMVs during January 2013. Observations filtered for QI2 > 80 and observed pressure below 700 hPa.**

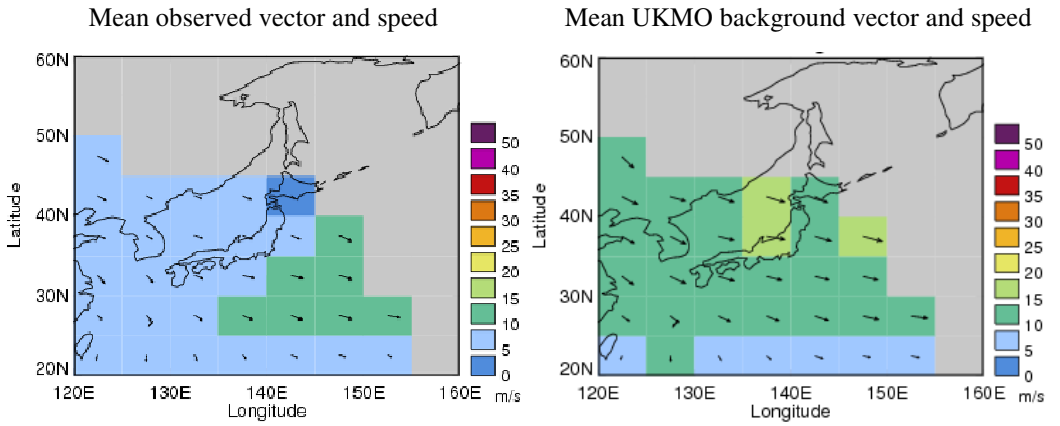


**Figure 34. Mean wind vectors (arrows) and wind speed (colour) for January 2013: FY-2E IR AMVs (left) and collocated Met Office model background winds (right). Observations filtered for QI2 > 80 and observed pressure below 700 hPa.**

### *Case study: 06z, 10 January 2013*

The surface pressure chart in Figure 35 shows the synoptic situation at 06:00 UTC on 10 January 2013. High pressure lies to the north and west of the Korean Peninsula whilst a deep low (minimum pressure 977 Mb) is anchored over the Bering Sea. A north or north-westerly flow is bringing cold air across the Sea of Japan. The 10:00 UTC visible image from MTSAT-2 (Figure 36) shows cloud streets aligned with the flow forming offshore from the Korean and Russian coast. The Japanese landmass is acting as a barrier to the flow but some cloud is able to pass through gaps and form further cloud streets downwind. A band of frontal cloud can be seen propagating south-eastwards near the bottom of the image.

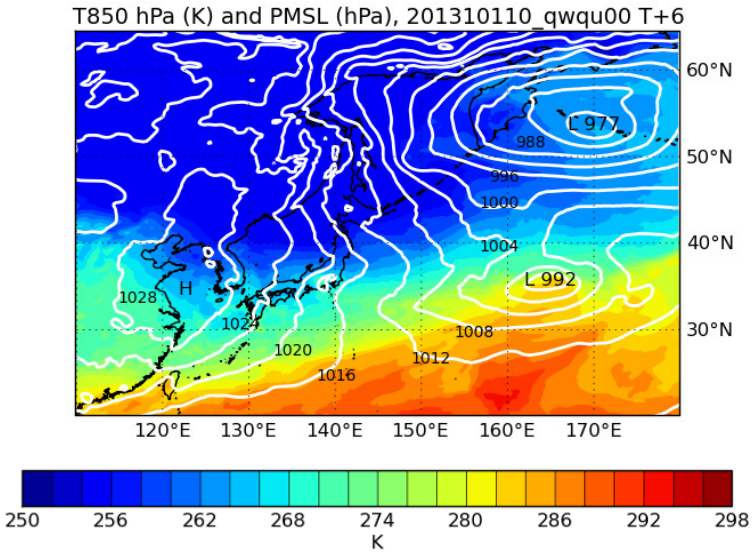


**Figure 35. Temperature at 850 hPa (filled contours) and MSLP (lines) for the 00:00 UTC T+6 forecast valid at 06:00 UTC 10 January 2013. Met Office global model forecast.**

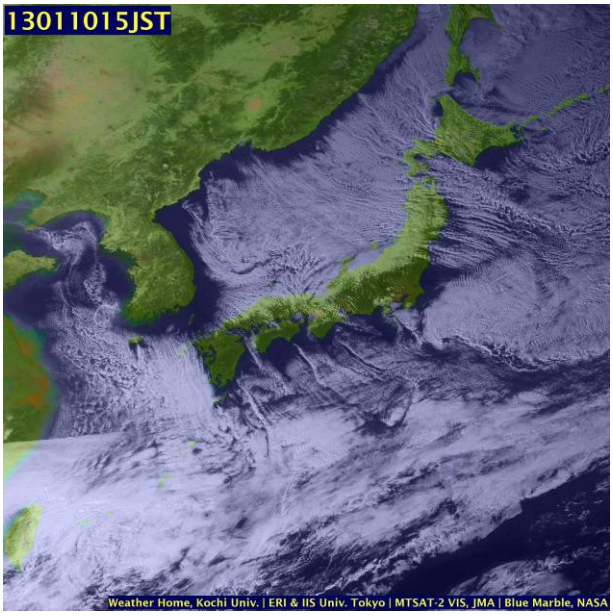


**Figure 36. MTSAT-2 visible image 06:00 UTC (JST = UTC+9 hrs) 10 January 2013.**

Figure 37 compares O-B wind speeds for both FY-2E and MTSAT-2 IR AMVs valid at 06:00 UTC. FY-2E has far fewer winds extracted, but those that are located over the Sea of Japan exhibit a significant negative speed bias often in excess of minus 8 m/s. AMV speeds are generally in the range 5-10 m/s from the NW (Figure 38) whereas model wind speeds are around 10 m/s faster. The model winds also tend to be from a more westerly direction. The majority of winds to the north of Japan have been assigned pressures in the range 720-820 hPa. A handful of vectors near the coast around 40°N, 130°E have been assigned lower (870-925 hPa) and show a reduced speed bias although not much agreement in direction. A group of northerly winds near 32°N, 124°E have also been assigned lower, below 900 hPa, and show better

vector agreement with the model. This indicates that the negative-biased observations may have been assigned too high. The model best-fit pressure estimates in the Sea of Japan that are well-constrained seem to confirm this as heights are 50-150 hPa lower in the atmosphere.

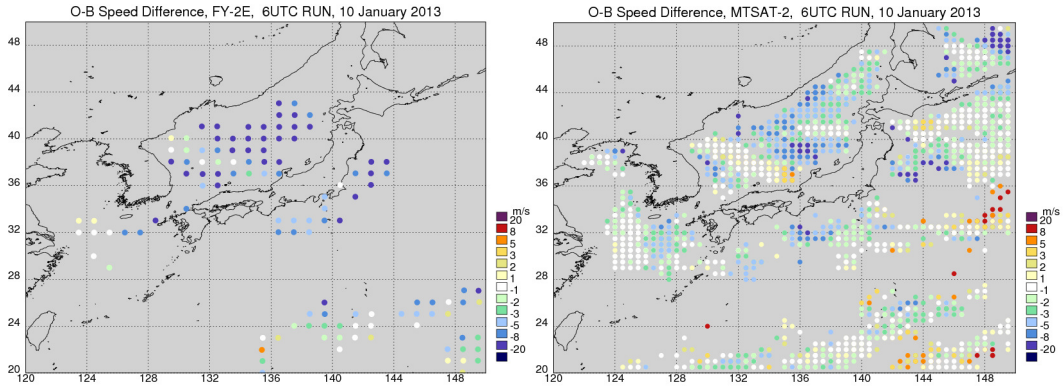


**Figure 37. Map of O-B speed bias for FY-2E (left) and MTSAT-2 (right) IR AMVs valid at 06:00 UTC 10 January 2013. Observations filtered for QI2 > 80 and observed pressure below 700 hPa.**

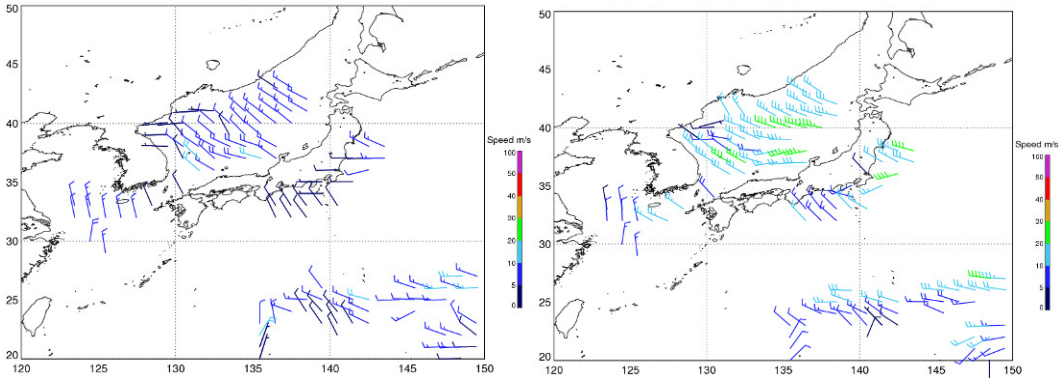


**Figure 38. AMV wind vectors (left) compared with collocated model winds (right). FY-2E IR AMVs valid at 06:00 UTC 10 January 2013. Observations filtered for QI2 > 80 and observed pressure below 700 hPa.**

For MTSAT-2 winds in the Sea of Japan, assigned pressures are in the range 850-900 hPa and the negative speed bias is less widespread. A swathe of winds near Korea show good agreement with model speeds. Model best-fit pressure estimates are not well-constrained for the band of negative biased AMVs near 40°N, 136°E as the model wants to put them too low (below 1000 hPa). Tracking (e.g. blocked flow due to orography) or model errors may be playing a role in this area.

## 4. Mid level updates

### Feature 2.8 and 2.9. Positive speed bias in the tropics, negative speed bias in extra-tropics

Feature background:

Two strong signals are seen in the O-B monitoring statistics at mid level: AMVs that are faster than the model in the tropics (Feature 2.8) and AMVs that are slower than the model in the extra-tropics (Feature 2.9).

Update:

The most important change since AR5 has been the introduction of the CCC method for the EUMETSAT MSG winds.

Figure 39 compares the IR 10.8μ winds for the month prior to the introduction of the CCC change and for the same month a year later. In August 2012 there is a very marked, widespread negative speed bias south of 20°S above 600 hPa (consistent with southern winter). The plot for August 2013 shows a number of important changes as a result of the CCC method. Firstly, there are many more winds being assigned to mid level (increase of around 100%) and the data gaps around 600-700 hPa have been filled. A significant positive impact of CCC is the reduction in magnitude and extent of the negative speed bias in the southern hemisphere extra-tropics. A negative impact is the increase in positive speed bias in the tropics (around 10-20°S in August 2013) which although it extends up to high level, tends to peak below 400 hPa.

A clearer picture of the longer term impact can be gained from examining time series of CGMS approved statistics as in Figure 40. These statistics differ from the NWP SAF statistics in that they are calculated using the QI with model first guess check. The time series show how the RMSVD and bias have changed through the implementation of the CCC method and also the switch to Meteosat-10. Note that a two month parallel period of CCC data (July-August 2012) has also been included here. In the southern hemisphere the improvements introduced with the CCC scheme are clear: RMSVD has reduced by about 4 m/s and mean speed bias is much closer to neutral. The northern hemisphere (not shown) also sees a reduction in RMSVD, but only during the winter months. In the tropics the RMSVD is slightly higher for the CCC data during the parallel period, but both RMS and bias increase markedly during the January-February peak that occurs each year. This annual

'spike' is largely related to problems assigning heights to winds over the Sahara as described in previous analysis reports (e.g. see update on Feature 2.8 in AR4).

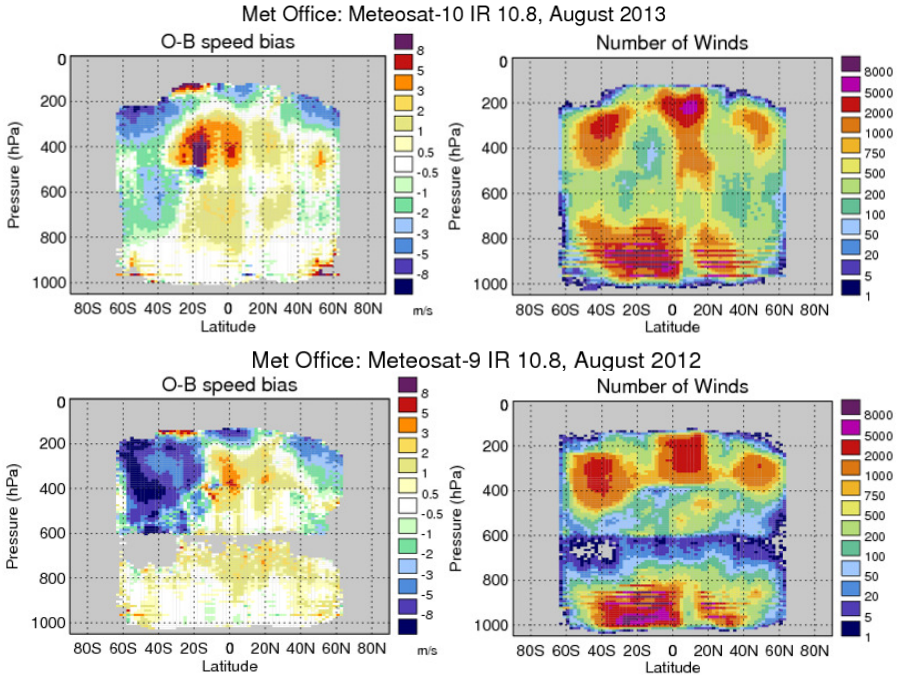


**Figure 39. O-B speed bias (left) and number of winds (right) for MSG IR 10.8 AMVs: Meteosat-10 from August 2013 (top) and Meteosat-9 from August 2012 (bottom). Observations filtered for QI2 > 80.**

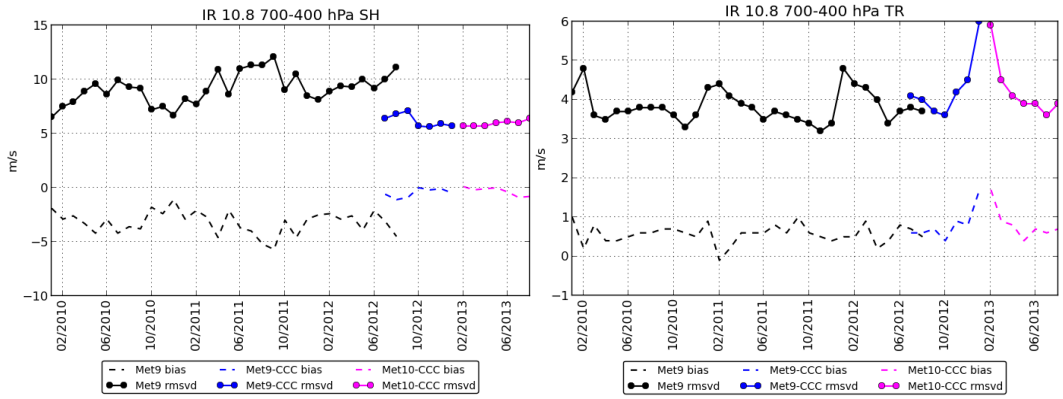


**Figure 40. Time series of RMSVD (solid line) and O-B speed bias (dashed line) for IR 10.8 AMVs. CGMS statistics shown for mid level winds 400-700 hPa between 90°S-20°S (left) and 20°S-20°N (right). Observations filtered for QI1 > 80 (with first guess check).**

A similar comparison for the cloudy WV 7.3μ winds before and after the CCC change is shown in Figure 41. In March 2012 there is a strong positive speed bias at mid level located around 5-30°N which extends from 400 hPa down to the lower limit of the AMV extraction at around 650 hPa. The remainder of the tropics also tends to show a positive speed bias. In March 2013, the positive speed bias is even more widespread and covers most of the region 40°S-40°N. Similar to the IR winds, there are more winds being assigned to mid level (175% increase) but the WV winds are

also now being extracted at much lower levels, in cases down to 1000 hPa. The zonal plots from April-September 2013 show data assigned even lower due to the use of the inversion height assignment scheme. This was subsequently disabled for the WV channels on 18 September 2013 and the zonal plots for October 2013 onwards show WV winds only extracted above 700 hPa. The longer term trends can be seen from the time series in Figure 42. In the southern hemisphere there is a clear improvement in RMSVD, both during the parallel period (1-2 m/s reduction) and subsequently with smaller 'peaks' during the winter months. This improvement is offset by an increase in mean speed bias by around 1 m/s. In the tropics and northern hemisphere there is an increase in both RMSVD and speed bias which is most evident during January and February 2013.

The statistics for the cloudy WV 6.2 channel (not presented here) show quite a marked degradation at mid level with the use of the CCC method with a positive speed bias of between +4 to +6 m/s across all latitude bands.

Overall, the implementation of the CCC method has had a mixed impact at mid level. There are improvements for the IR winds in the extra-tropics but slightly offset by some degradation in the tropics. The cloudy WV winds show a more general degradation in terms of speed bias and this could be considered as a separate feature for investigation in future analysis reports.

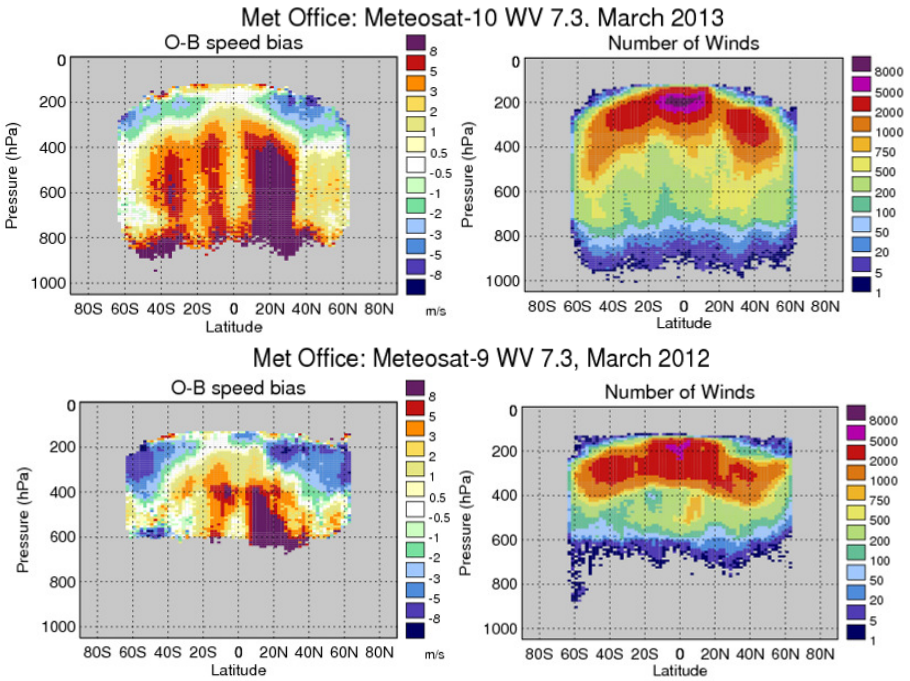


**Figure 41. O-B speed bias (left) and number of winds (right) for MSG cloudy WV 7.3 AMVs: Meteosat-10 from March 2013 (top) and Meteosat-9 from March 2012 (bottom). Observations filtered for QI2 > 80.**

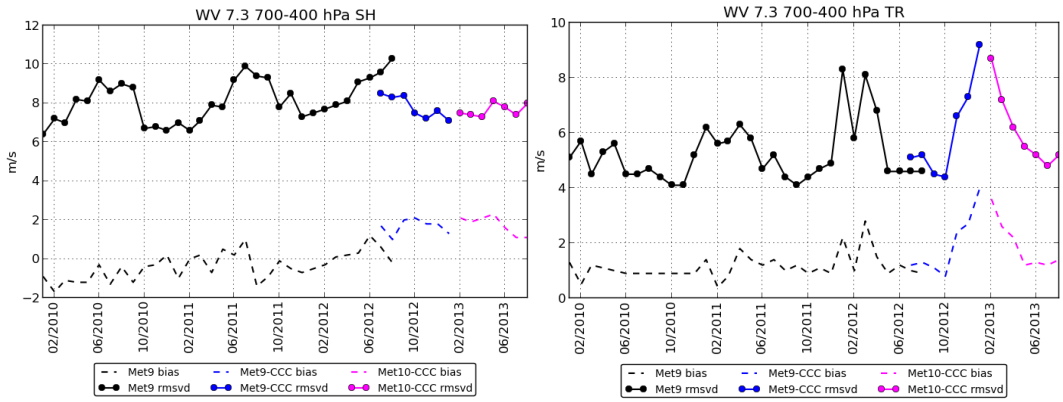


**Figure 42. As Figure 40 but for mid level cloudy WV 7.3 AMVs.**

## 5. High level updates

### Feature 2.10. Jet region negative speed bias

Feature background:

The dominant signal in the O-B monitoring statistics at high level is a negative speed bias located in the extra-tropics. The bias is usually associated with the position of the jet stream and hence peaks in the winter months. It is often more marked in the northern hemisphere. Previous analyses have suggested the main causes to be 1) height assignment error in high wind shear environments, 2) representative errors and 3) errors in the tracking step.

Update:

***MTSAT-1R/2***

The negative bias continues to be very pronounced for the MTSAT IR channel in the northern hemisphere where there are strong peaks in both RMSVD and speed bias in December/January each year. The southern hemisphere is affected to a lesser degree and reflects the difference in the relative strength of the jet stream. The MTSAT WV winds are slightly unusual in that the data generally show more of a positive speed bias (see update in AR4).

***FY-2E***

The FY-2E IR winds generally show a negative speed bias year-round in both extra-tropics versus the Met Office and ECMWF models (e.g. see Figure 43). However it is clear from the NWP SAF plot archive that substantial improvements have been made

to the quality of the winds since 2010 (see also Cotton, 2013). The mixed WV winds generally show much less of a negative speed bias in comparison to the IR.

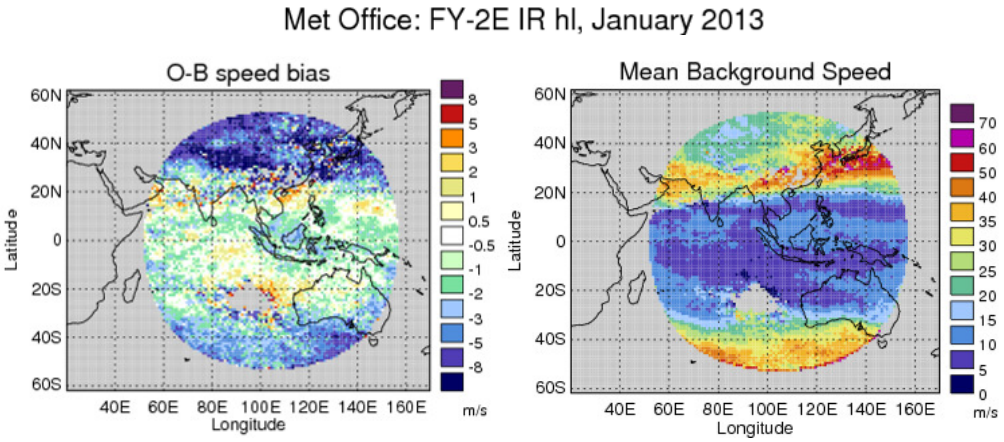


**Figure 43. O-B speed bias (left) and mean collocated Met Office background speed (right) for MTSAT-2 IR AMVs from January 2013. Observations filtered for QI2 > 80.**

For the IR winds, Figure 43 shows that there is a strong negative speed bias signal near Japan which coincides with the location of the fastest wind speeds according to the model. The plot also shows another strong negative bias signal to the north east of India (around 80-100°E, 30-40°N) which only coincides with moderately strong model speeds of around 20-30 m/s. This signal persists for a large portion of the year but is most significant between October and May. In contrast, there are AMVs in significantly stronger wind regimes (e.g. N Arabian Sea) which exhibit a more neutral wind speed bias. Hence, the bias is not purely wind speed dependant.

Figure 44 confirms a negative speed bias is present in January 2013 across all wind speed regimes in the northern hemisphere. However the relationship is not linear as there is clearly a local 'peak' in the bias for moderate wind speeds around 30 m/s. This would appear to match the characteristics of the bias seen in the maps to the NE of India as described above. Above 60 m/s the negative speed bias tends to increase with speed once more. By contrast, the O-B speed bias in the southern hemisphere (not shown) displays a much more linear relationship.

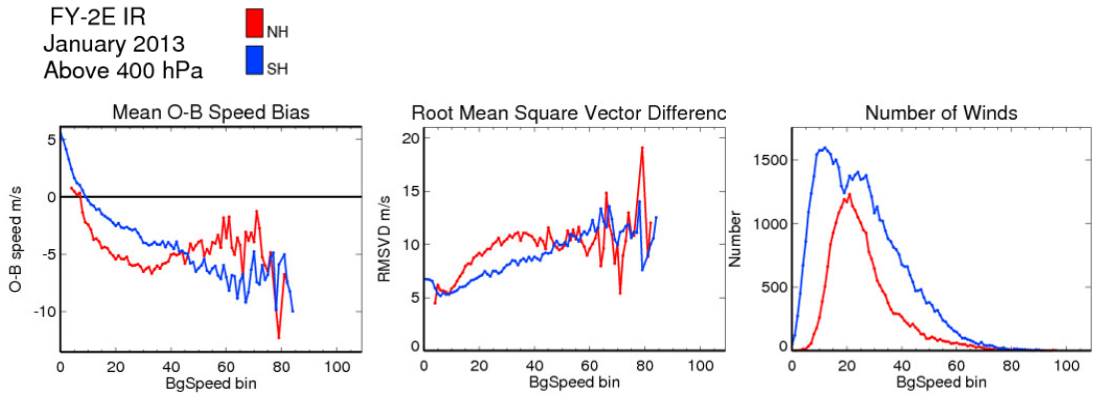


**Figure 44. O-B speed bias (left), RMSVD (middle) and number of winds (right) as a function of collocated model wind speed. Red is 20°N-90°N, blue is 20°S-90°S. MTSAT-2 IR AMVs from January 2013 filtered for QI2 > 80.**

Figure 45 shows the difference between AMV and model wind speeds for FY-2E IR winds extracted between 15:00 UTC and 21:00 UTC on 31 January 2013. The map shows that the AMVs are slower than the model over a wide area but the largest difference is found in a band between 30-36°N. Here the AMVs are much slower (not seen in the forecast) and as a result O-B's are in excess of minus 8 m/s. Further north there are AMVs with a more neutral speed bias located around 76-84°E.

Figure 46 shows that the worst of the negative speed bias is associated with forecast wind speeds of only around 15-20 m/s. A curve of faster wind speeds (shaded green) are located further south and the southern edge of these shows good vector agreement with the model. A group of fast winds (pink and red shading) located near 23°N 72°E with speed up to 55 m/s are likely part of the jet stream and again show good agreement with the model.

It is noticeable from the map of pressures in Figure 45 that the band of negative-biased observations between 30-36°N have been assigned higher in the atmosphere than the surrounding observations. Assigned pressures are in the range 230-300 hPa whilst model best-fit pressure estimates are reasonably well constrained to 350-550hPa. This suggests the large negative bias could be due to the AMVs being assigned too high.

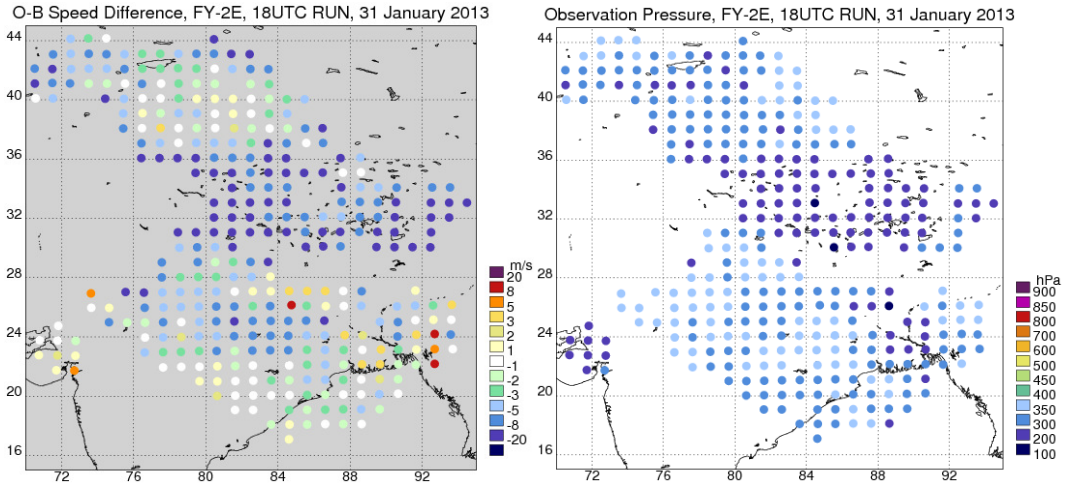


**Figure 45. Map of O-B speed bias (left) and assigned AMV pressure (right) for FY-2E IR AMVs valid at 18:00 UTC 31 January 2013. Observations filtered for QI2 > 80 and observed pressure above 400 hPa.**

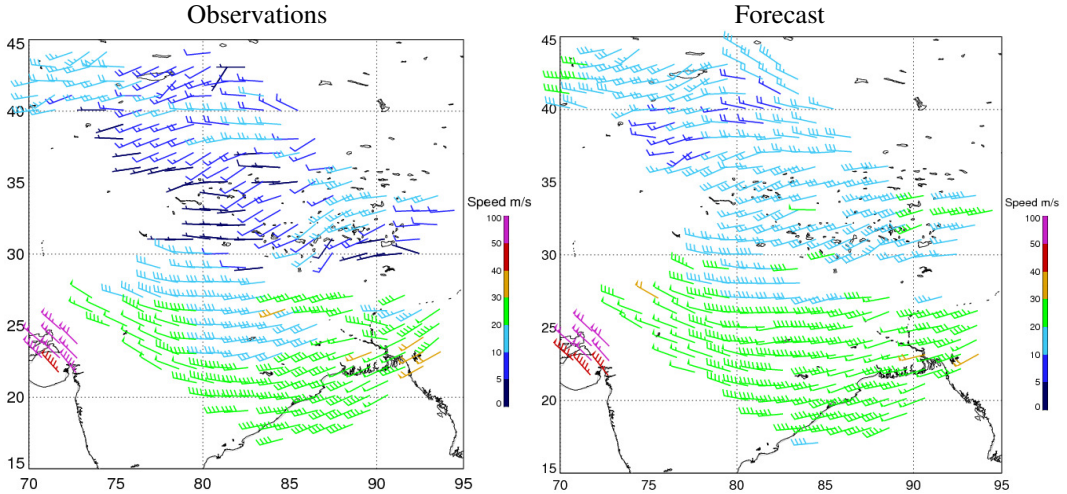


**Figure 46. AMV wind vectors (left) compared with collocated model winds (right). FY-2E IR AMVs valid at 18:00 UTC 31 January 2013. Observations filtered for QI2 > 80 and observed pressure above 400 hPa.**

The WV channel wind speed are similar to the IR winds in this case, but assigned heights for the band of negative-biased winds are lower at around 300-400 hPa. The very few collocated Meteosat-7 IR and FY-2E IR winds for this day/area show the Meteosat-7 winds to be lower in the atmosphere by around 50 hPa. Both results would reaffirm that the FY-2E IR winds have been assigned too high.

Why might the FY-2E AMVs, and the IR winds in particular, have been assigned too high in the problem area? Figure 47 shows the O-B speed bias plotted over a map of topography. The strongly biased AMVs have been retrieved over the high terrain of the Tibetan Plateau and in this case there is a fair matchup between the observed AMV bias and elevations above 3 km. As previously noted, north of 36°N there is a group of AMVs with more of a neutral speed bias and this roughly coincides with a

drop in surface elevation down to 1-2 km. The scatter plot of speed bias versus elevation in Figure 48 shows a fair degree of correlation and that the worst of the negative bias occurs for observations over 4500 m. The Met Office surface pressure forecast for the highest elevations (Figure 48, right) shows pressures as low as 515 hPa. This means that the range of model best-fit pressure estimates for the IR winds discussed earlier (350-550 hPa) are in fact very close to the surface.

The IR imagery for this case (Figure 49) shows bands of cirrus flowing over the cold surface of the plateau. The colour enhancement applied for brightness temperatures colder than 245 K helps to distinguish the cloud tops: coldest temperatures are around 216 K (-57°C) for those located over the plateau. However some of the yellow shading of the enhancement also picks out the surface of the plateau. The high topography is also clearly visible in the corresponding WV channel imagery.

For this particular case it is possible that the high, cold surface of the plateau is playing a part in the AMVs being assigned too high. This could be due to an error in the NWP temperature profile or skin temperature used in the radiative transfer model. The presence of topography in the WV channel image could be causing problems with cloud detection and also the observed IR/WV relationship used for height assignment of semi-transparent clouds. The tracking of surface features may be another reason for the slower AMVs over the plateau.

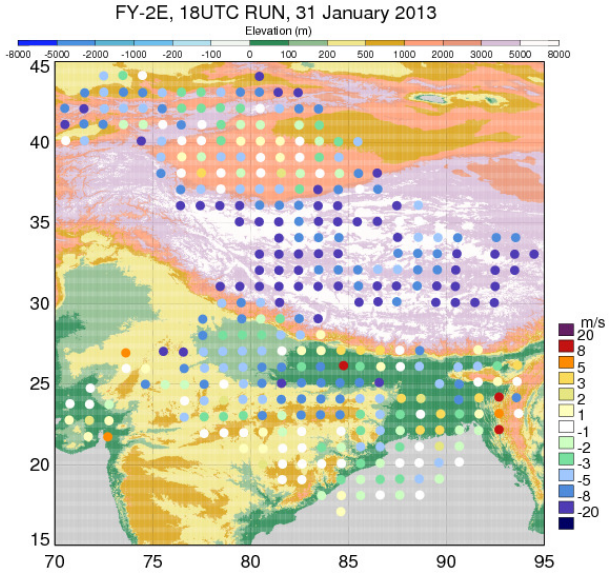


**Figure 47. As Figure 45 (left) but O-B speed bias overlain on a map of topography.**

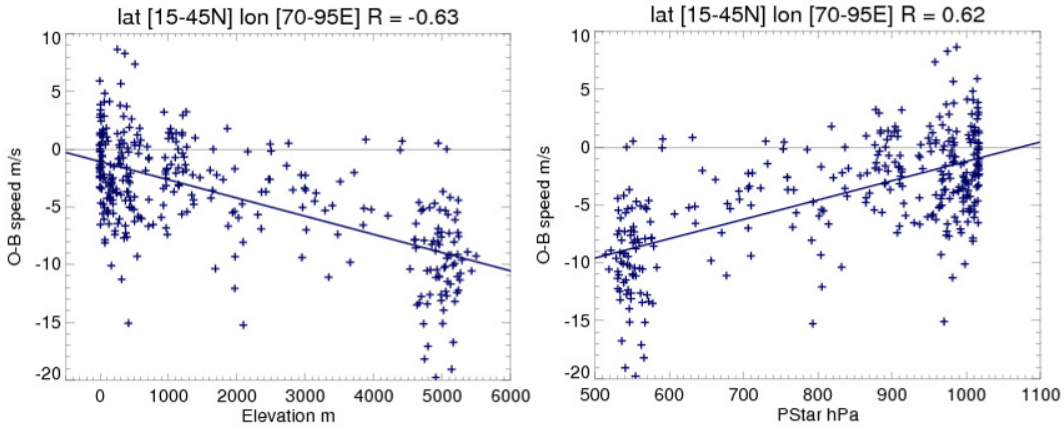


**Figure 48. O-B speed bias scatter plot versus surface elevation (left) and Met Office surface pressure (right). Data plotted is as per Figure 47.**

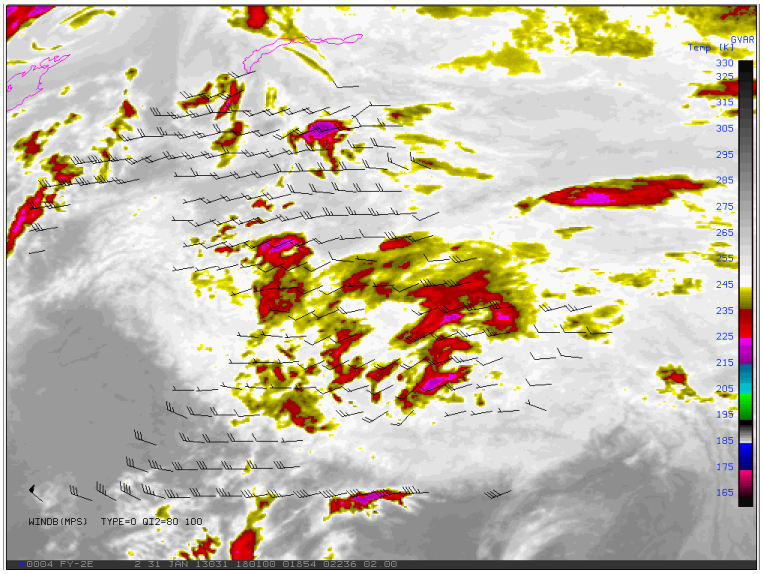

**Figure 49. McIDAS visualisation of colour-enhanced FY-2E IR imagery at 1801 UTC, 31 January 2013 together with IR wind vectors. Observations filtered for QI2 > 80 and observed pressure above 400 hPa.**

### *MSG*

As for the mid level winds, the most important change since AR5 has been the introduction of the CCC method for the MSG winds.

Figure 50 compares the IR 10.8μ winds for the month prior to the introduction of the CCC change and for the same month a year later. As already seen for the mid level data, in August 2012 there is a very marked negative speed bias south of 20°S consistent with southern hemisphere winter. The plot for August 2013 shows the negative wind speed bias in the southern hemisphere extra-tropics has been greatly reduced in magnitude and extent. The CGMS time series in Figure 51 show how the

RMSVD and bias have changed through the implementation of the CCC method and also the switch to Meteosat-10. There is a substantial improvement in the statistics in both extra-tropics. The CCC impact is most evident in the southern hemisphere as the change was made just after southern winter. Here the RMSVD and speed bias are reduced in magnitude by around 2 m/s. A similar level of improvement can be seen for the winter 'peak' in RMSVD in the northern hemisphere.

The cloudy WV 7.3μ channel statistics are similarly improved with the CCC method, but the WV 6.2μ channel shows little change in RMSVD.

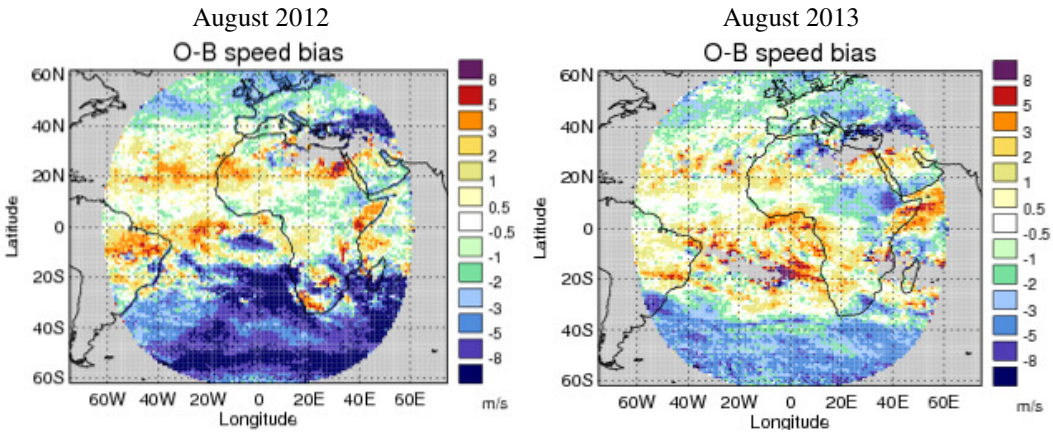


**Figure 50. O-B speed bias for MSG IR 10.8 AMVs: Meteosat-9 from August 2012 (left) and Meteosat-10 from August 2013 (right). Observations filtered for QI2 > 80 and above 400 hPa.**

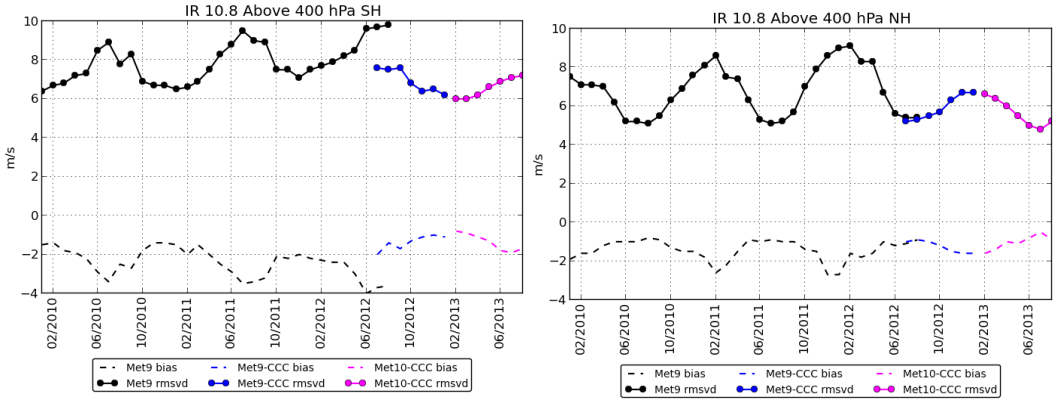


**Figure 51. Time series of RMSVD (solid line) and O-B speed bias (dashed line) for IR 10.8 AMVs. CGMS statistics shown for winds above 400 hPa between 90°S-20°S (left) and 20°S-20°N (right). Observations filtered for QI1 > 80 (with first guess check).**

## Feature 2.13. Tropics positive speed bias

Feature background:

A positive O-B speed bias is observed in the tropical region of the upper troposphere for most satellite-channel combinations. The bias tends to be more pronounced in the WV channels. Previous case studies have highlighted difficulties in: a) tracking and assigning heights to changing, linear cloud tracers, b) height assignment of cloud edges in regions of wind shear.

Update:

***MSG***

Since the last analysis in AR5 the CCC method has been introduced for the MSG winds. The time series in Figure 52 show how the RMSVD and bias have changed through the CCC change and also the switch to Meteosat-10 for the IR 10.8μ and WV 6.2μ winds. The parallel period of CCC data shows an improvement in vector difference and speed bias for both these channels. In particular, the positive speed bias for WV 6.2μ is reduced by around 0.3-0.4 m/s but remains worse in comparison to the IR. The cloudy WV 7.3μ channel (not shown) shows no impact on speed bias but some improvement in RMS vector difference.

The NWP SAF map plots for the IR 10.8μ channel before and after the change suggests that the positive speed bias is now less widespread. There also appears to be a small reduction in the occurrence of linear-shaped positive bias features which are often associated with cloud edges. This could be due to these pixels being selected less frequently for height assignment under the CCC scheme.

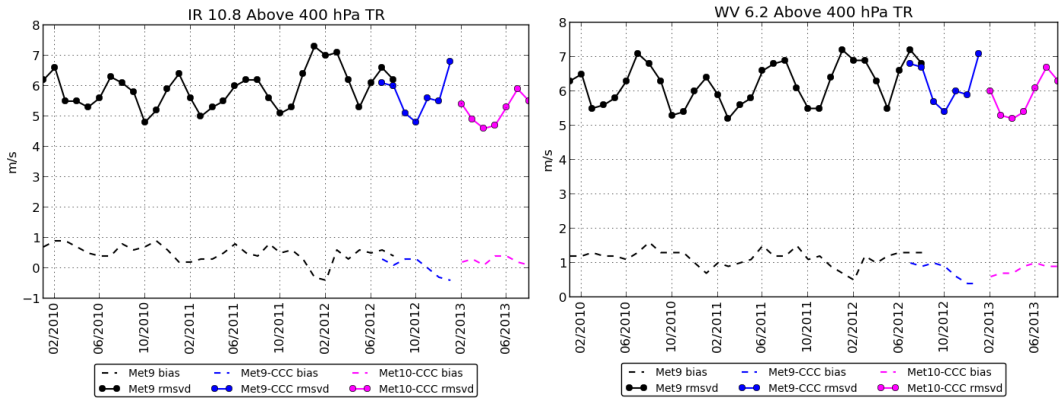


**Figure 52. Time series of RMSVD (solid line) and O-B speed bias (dashed line) for IR 10.8 AMVs (left) and WV 6.2 AMVs (right). CGMS statistics shown for winds above 400 hPa between 20°S-20°N. Observations filtered for QI1 > 80 (with first guess check).**

***Meteosat-7***

No changes since AR5.

***FY-2E***

The tropical IR winds exhibit a negative speed bias of between 1-2 m/s at high level. The mixed WV channel winds appear more neutral.

***MTSAT-1R/2***

Whilst the IR channel winds appear quite neutral the cloudy WV winds show a more widespread positive speed bias.

***GOES-13/15***

GOES-13 IR and cloudy WV monitoring shows an unusually marked area of positive speed bias in January 2012, located 80ºW-105ºW between 0-20ºS. November and December 2012 also show a similar feature around the edge of a cloud-free region, but only in the WV channel. The hourly GOES-13 winds being monitored offline at this time show a reduced bias in December 2012 due to an absence of winds extracted in that region (larger cloud free-area).

## Feature 2.14. High-troposphere (above 180 hPa) positive speed bias

Feature background:

A positive speed bias for Meteosat-7, MSG and GOES (unedited data) AMVs assigned heights high in the upper troposphere. The bias may be due to a 'high' height assignment bias. There is a seasonal dependence affecting the EUMETSAT data: a positive bias can be observed between October-April, the rest of the year is dominated by a negative speed bias (see update on Feature 3.2).

Update:

***Meteosat-7***

This feature remains present for Meteosat-7 WV winds extracted above 180 hPa in the tropics, e.g. zonal O-B plot for March 2013. The bias only exists for part of the year, usually October- April. The IR winds are less affected as far fewer winds are extracted this high.

***MSG***

AMVs from MSG are extracted above 200 hPa over a greater latitudinal area compared to MFG and the positive speed bias can be seen to extend to 40º N/S, e.g. see zonal plots for Oct 2012. The cloudy WV and IR channels are equally affected over the same October-April period as MFG.

***GOES***

The feature is very prominent year-round in the unedited GOES-13/14 IR and cloudy WV channel data. The final edited operational products and GOES hourly winds are not affected.

## Feature 3.2. High-troposphere (above 180 hPa) negative speed bias in Tropical Easterly Jet

Feature background:

A negative speed bias for Meteosat-7 and MSG winds in the high-troposphere of the tropics between June and September. This seasonal feature has been shown to coincide with the presence of the Tropical Easterly Jet (TEJ) but it has not previously been investigated whether this is due to model or observation error.

Update:

Figure 53 compares August 2013 mean vector and speed differences for Meteosat-10 IR 10.8μ and Meteosat-7 WV AMVs collocated with Met Office global model background estimates. Only observations assigned heights above 200 hPa have been considered. The upper troposphere model-mean wind field shows the TEJ stretching from SE Asia to Eastern Africa with speeds in excess of 30 m/s centred around 5-10°N. This upper level easterly is an important component of the Asian Summer Monsoon and peaks from June-September, the same months in which the AMV speed bias is observed. The mean wind field derived from Meteosat-7 and MSG AMVs describes a much weaker easterly with O-B differences widely greater than 5 m/s (locally 8 m/s). This is particularly notable over the southern and western portion of the TEJ. Equivalent plots against the ECMWF background (not shown) reveal a similar pattern of O-B speed bias but perhaps slightly smaller in magnitude.

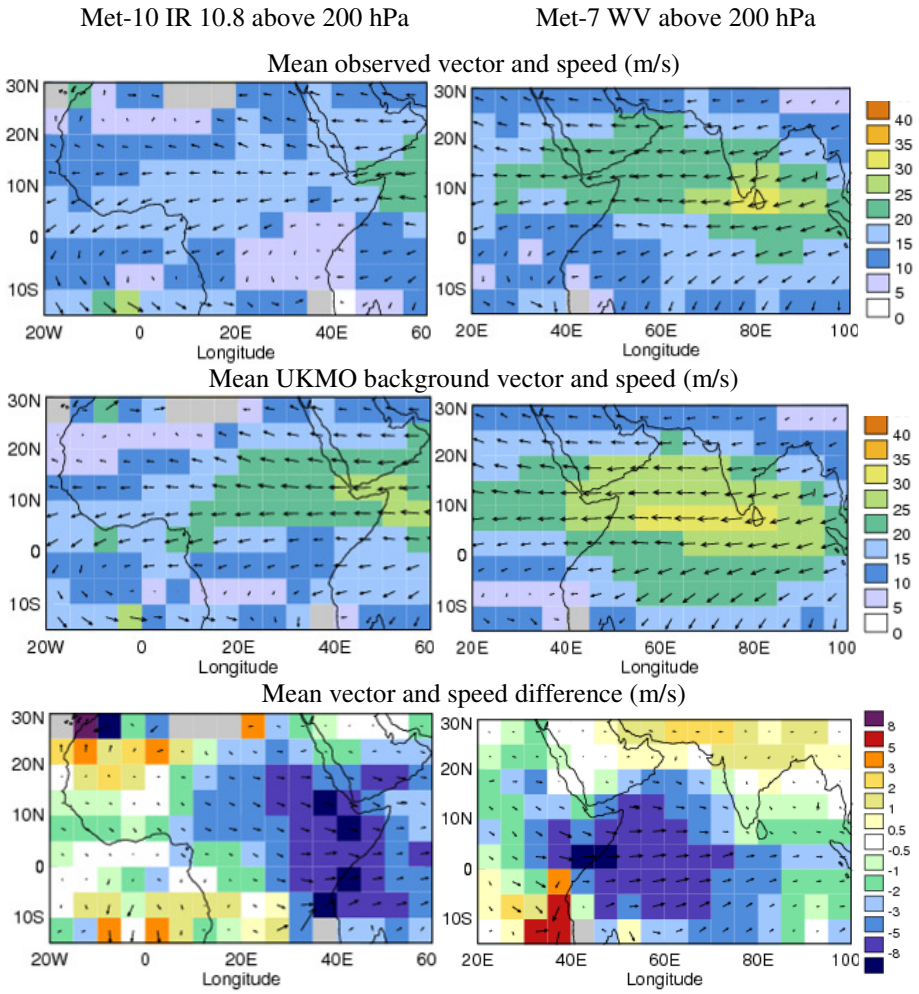


**Figure 53. Mean wind vectors (arrows) and wind speed (colour) for August 2013: Met-10 IR 10.8 AMVs (left) and Met-7 WV AMVs (right). Mean AMV (top), mean collocated UKMO background (middle) and mean difference (bottom). Observations filtered for QI2 > 80 and assigned pressure above 200 hPa.**

Comparison of zonal O-B speed bias plots on the NWP SAF website confirms that the negative speed bias tends to be larger in the Met Office system indicating a possible contribution from model error. Figure 54 compares the mean Met Office and ECMWF wind analyses at 150 hPa, the level at which the TEJ peaks in August 2013. Wind speed differences between the two models are very large in equatorial East Africa and the West Indian Ocean region centred on 50°E. Met Office mean wind speeds are up to 10 m/s faster than the ECMWF analysis and appear too strong to the south of the jet core. The geographical location of the analysis difference closely matches the bias as described by the Meteosat-7 AMVs in Figure 53. At 200 hPa the magnitude of the analysis difference is smaller, but the sign reverses with ECMWF having a stronger easterly by up to 6 m/s in the same region (Figure 55). This reversal suggests a possible error in the vertical wind distribution.

The vertical cross section in Figure 56 compares the mean zonal wind analyses at 50°E, the longitude where the wind speed differences are greatest. This shows that there is some vertical displacement error e.g. see the -10 m/s contour line around the equator region where the Met Office easterly appears too high. However there is also a large difference is in the strength/size of the jet core with the Met Office analysing a faster easterly which extends much further south (e.g. compare -30 m/s contour).

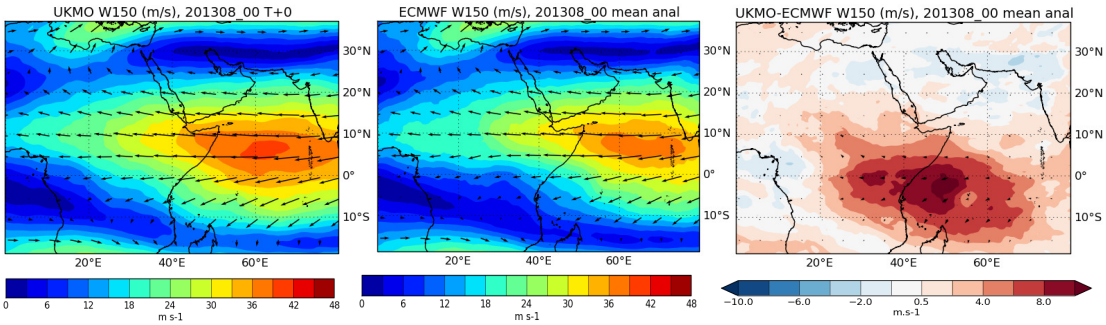


**Figure 54. Mean analysed Met Office (left) and ECMWF (middle) winds at 150 hPa for August 2013 and the mean vector (arrow) and speed (shading) difference (right).**

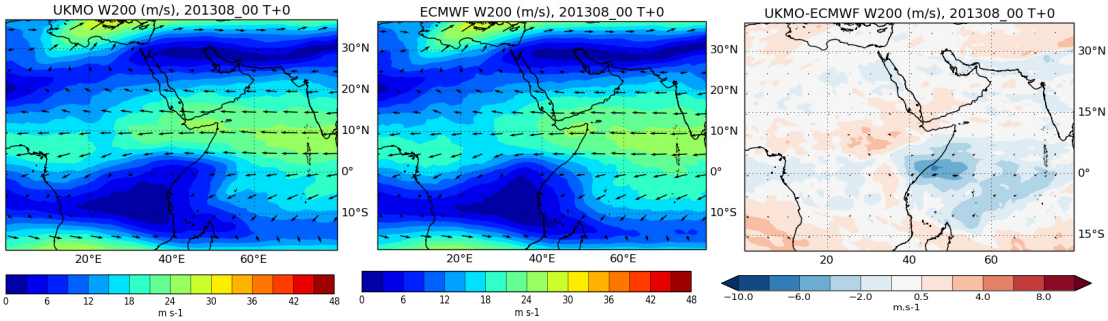


**Figure 55. As Figure 54 but for 200 hPa.**

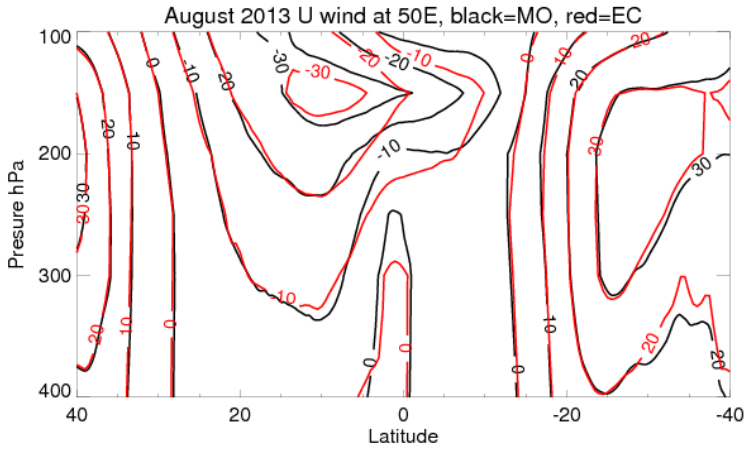


**Figure 56. Cross section of the mean zonal (U) wind component at 50°E: Met Office analysis (black) and ECMWF analysis (red).**

Differences between the ECMWF and Met Office models persists through forecast fields out to 5 days, although not as large as in the analysis. Figure 57 shows the drift

in the Met Office and ECMWF forecasts away from their respective analyses for different lead times. In the region circled (where the Met Office analyses are much faster than ECMWF) the Met Office forecasts winds tend to weaken in strength (blue shading) with increasing forecast range. By day 5 the southerly portion of the TEJ has been weakened by 4-6 m/s suggesting the issue is an analysis problem rather than a forecast model/background one. The ECMWF forecasts on the other hand tend to strengthen in the first 24 hours which may explain why, although the models are very different at T+0, the O-B's tend to be more similar. The plots also show that both Met Office and ECMWF forecasts move towards a much faster (red shading) exit of the TEJ over West Africa (westwards of 20ºE and south of 10ºN).

Overall, there is strong evidence that the negative speed bias observed in the NWP SAF monitoring is in large part due to an excessively strong representation of the TEJ in the Met Office analysis. Improving the assimilation of AMVs in this area could help to reduce the analysis error.

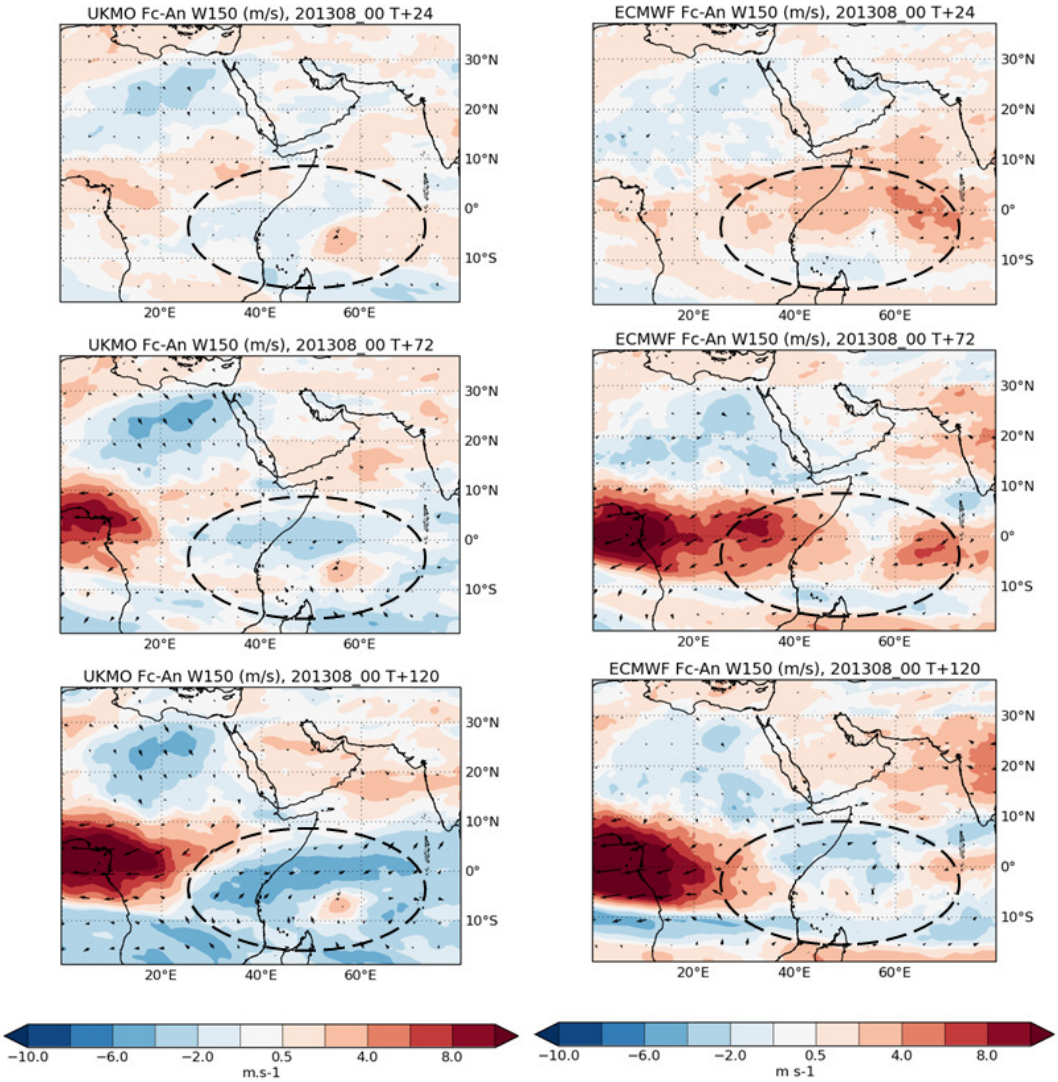


**Figure 57. Mean 150 hPa wind vector and wind speed forecast error for Met Office (left) and ECMWF (right) verified against own analysis. T+24 forecast (top), T+72 forecast (middle) and T+120 forecast (bottom). Data from August 2013.**

## Feature 3.3. GOES-W bias change at 180°

Feature background:

A known issue with the AMVs derived from GOES West: artificially high wind speeds west of the 180° meridian. This has been linked to a problem with the autoeditor step in the NESDIS processing. As reported in AR5 this bias is expected to be fixed when the derivation updates tied-in with the hourly GOES data are operational.

Update:

An extreme occurrence of this bias was flagged by the Met Office monitoring system on 17 February 2013. Figure 58 compares the observed GOES-15 wind vectors with collocated Met Office background wind vectors at the observation location and height (the island at the base of the image is the North Island of New Zealand). The AMVs

derived in a band between 30°S and 25°S are anomalously fast when compared to the forecast wind speeds. AMV speeds are as a high as 70 m/s and O-B speed differences are extreme: in excess of +45 m/s. Most AMVs faster than 30 m/s have been assigned to 275 hPa. The hourly GOES data in this case show similarly fast observed wind speeds, but the O-B speed bias is much reduced (order of +5 m/s) due to the winds being assigned at 200 hPa. The bias in the operational data at this time is likely due to an erroneous pressure adjustment.

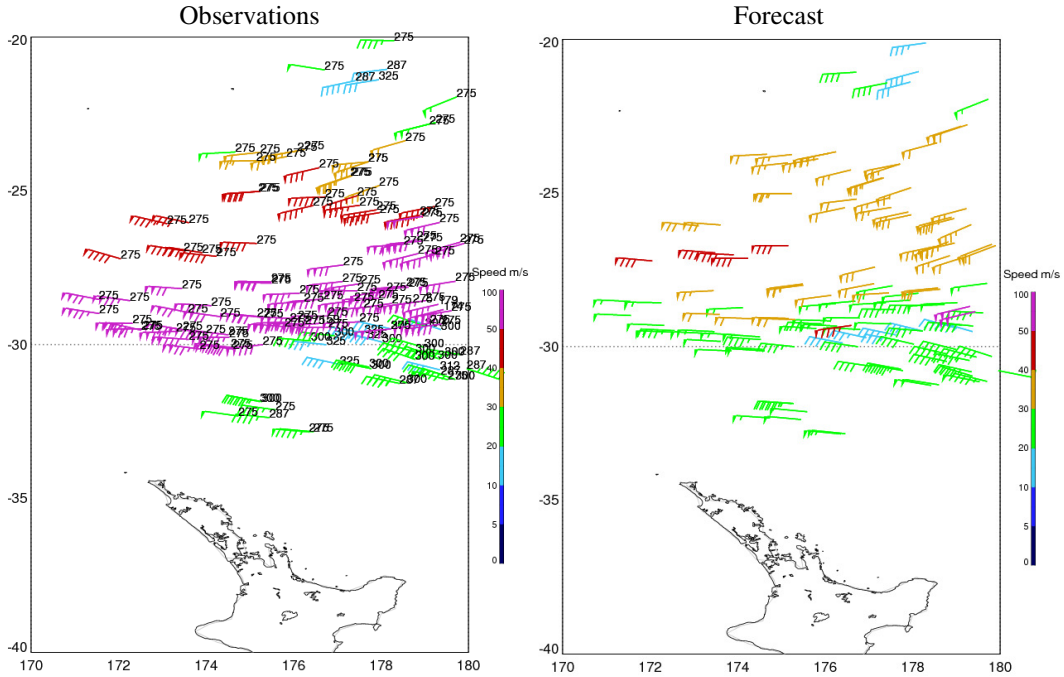


**Figure 58. AMV wind vectors and assigned pressure (left) compared with collocated model winds (right). GOES-15 IR AMVs valid at 00:00 UTC 17 February 2013. Observations filtered for QI2 > 80 and observed pressure above 400 hPa.**

## Feature 4.2. GOES negative bias in tropical Pacific

### Feature background:

Most AMV data sets at high level have a positive speed bias in the tropics (see Feature 2.13) but AMVs from GOES West instead exhibit a negative speed bias from December to April. Model errors are thought to contribute to the O-B signal which has also previously been shown to vary from year to year indicating some synoptic dependence.

### Update:

Met Office monitoring plots confirm this feature is still present for GOES-15 IR winds e.g. between December 2012 and March 2013. Time series plots (Figure 59)

demonstrate the seasonal nature of the bias, 'peaking' in northern winter. Initially the O-B statistics look worse following the transition from GOES-11 to GOES-15 but this may be incidental to the change in satellite. Although present in the WV data the magnitude of the bias is smaller.

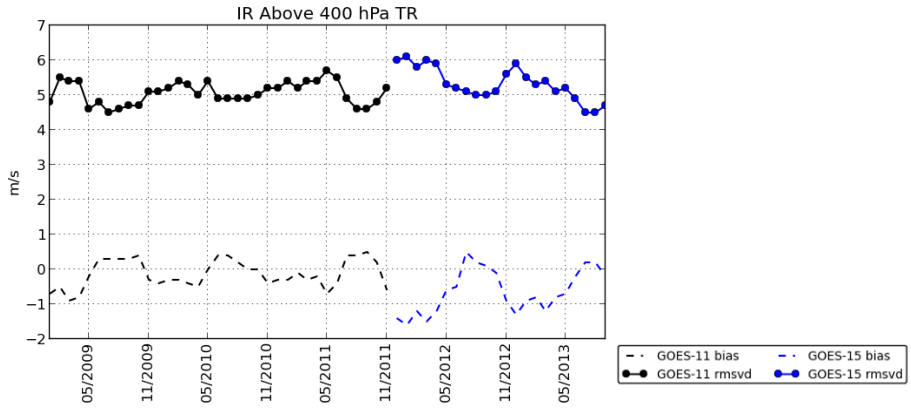


**Figure 59. Time series of RMSVD (solid line) and O-B speed bias (dashed line) for GOES West IR AMVs above 400 hPa, between 20°S-20°S. Observations filtered for QI1 > 80 (with FG check).**

The bias is not specific to GOES-15 as it also appears in the GOES-13 data covering the Eastern Pacific. In some months it can also be seen extending into the Atlantic (e.g. see January 2013) but in general this feature is much more persistent and widespread over the Pacific. Figure 60 compares the O-B speed bias for GOES-15 IR winds versus Met Office and ECMWF forecasts during February 2013. The Met Office plots shows a prominent negative speed bias running along an axis which crosses the equator at around 130-140°W. O-B's are widely in excess of 3 m/s in magnitude but in some cases exceeding minus 5 m/s. When the AMVs are compared to the ECMWF model background we observe a much reduced bias. This indicates that in this case there is a significant error contribution from the Met Office model.

The presence of model error is verified by Figure 61 which compares the mean Met Office and ECMWF wind analyses at 250 hPa for this month. The mean upper level circulation shows that the speed bias is located in the vicinity of moderate westerlies or north-westerlies which cross the equator at around 120-140°W. The equatorial flow appears to bridge the mid-latitude westerlies in both hemispheres due to an incursion from the North Pacific deep into the tropics. This feature of the Eastern Pacific circulation is often referred to as a 'westerly duct' and it allows the propagation of mid latitude (Rossby) waves in the upper troposphere (Webster and Holton 1982). The duct is most pronounced during northern hemisphere winter and is caused by the development of mid-Pacific troughs in the sub-tropics of both hemispheres (Murakami and Wang, 1993). The model difference plot in Figure 61

shows that in the westerly duct the mean Met Office analysed wind speed is quite widely 2 m/s stronger than ECMWF. This suggests that model error is contributing at least half of the observed O-B signal.

The GOES hourly winds product (which also includes some derivation changes) was being monitored offline at this time and the negative bias in the tropics is still very prominent, although marginally reduced in magnitude. Although this suggests the presence of some derivation error, the dominant error source in this case would appear to be the upper level circulation of the Met Office model in the Eastern Pacific. As shown by Figure 62 there is a strong (negative) correlation between the strength of the forecast zonal wind in the upper troposphere and the zonal speed bias versus the AMVs. During periods of strong westerlies (positive u) we observe a negative zonal wind bias, but when the flow is (briefly) easterly there is near-zero bias.

It should be noted that maps of O-B speed bias for other winter months do not show such a clear link between the bias and differences in the Met Office and ECMWF models.

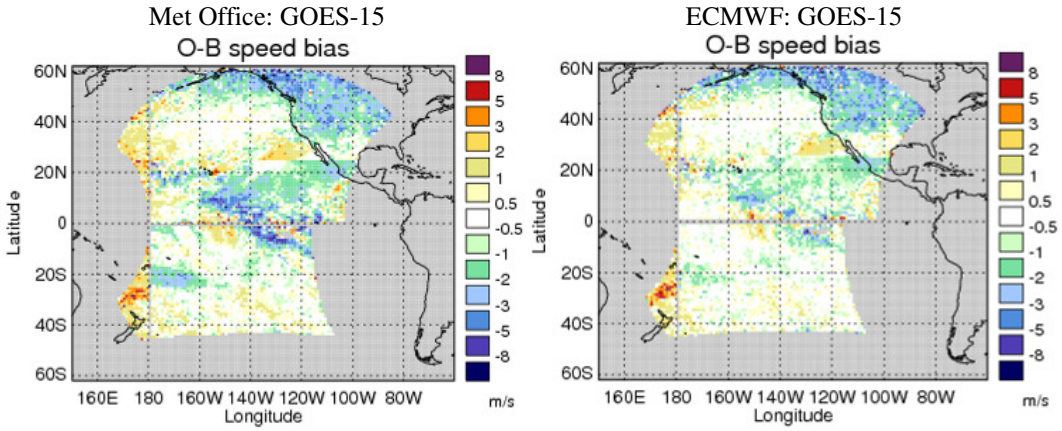


**Figure 60. Map of O-B speed bias for GOES-15 IR AMVs during February 2013: against the Met Office model (left) and ECMWF model (right). Observations filtered for QI2 > 80 and observed pressure above 400 hPa.**

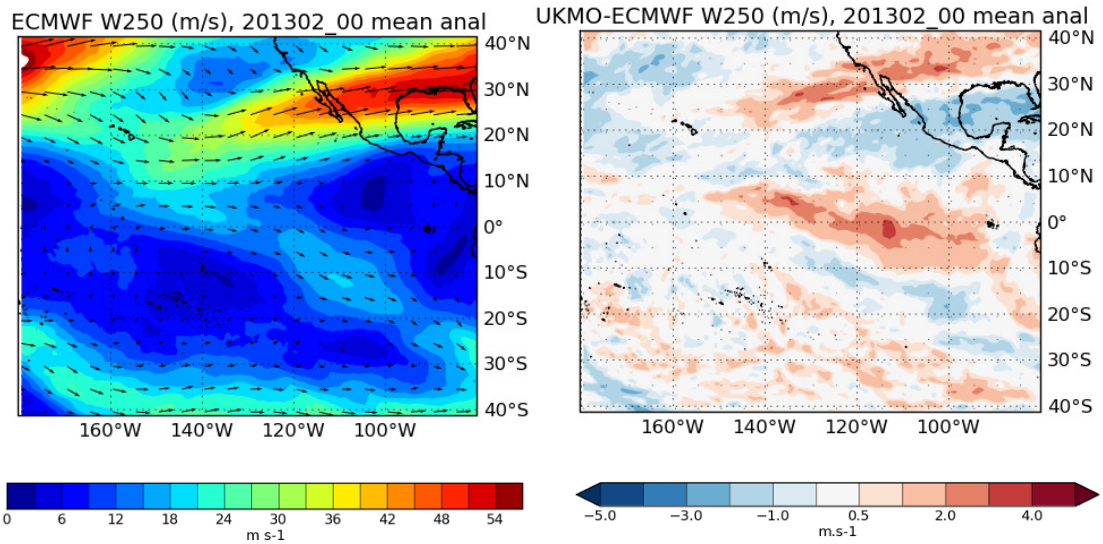


**Figure 61. Mean analysed ECMWF winds at 250 hPa for February 2013 (left) and the wind speed difference compared to the Met Office model (right). Note that the paired positive/negative wind speed bias north/south of 30°N is due to a small shift in the analysed position of the subtropical jet.**

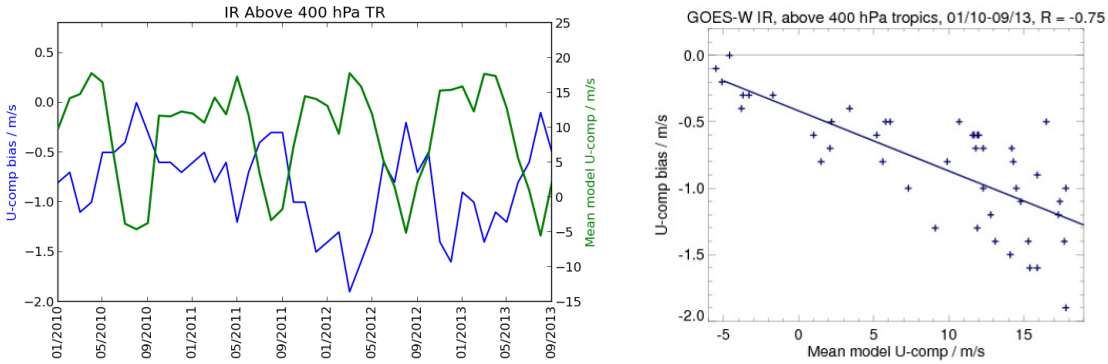


**Figure 62. Left: monthly time series of the mean O-B zonal wind component bias (blue) and mean Met Office zonal wind component (green) - note the different scales. Right: the same data as a scatter plot. GOES West IR AMVs above 400 hPa, between 20°S-20°S. Observations filtered for QI1 > 80.**

## Feature 5.3. MTSAT tropical cyclone speed bias

### Feature background:

MTSAT WV winds generally show a positive speed bias at high level, but more marked features can be seen in the NW Pacific basin during the tropical cyclone season. A case study from 2011 showed problem AMVs tracking cirrus outflow from a passing typhoon and a speed bias resulted from AMVs being assigned too low.

### Update:

This feature remains present, but less pronounced in the NWP SAF map plots for 2012 and 2013. The clearest signal from recent data can be seen in October 2013 to the south west of the Philippines and this coincides with an increase in tropical

cyclone activity – 7 typhoons were active during this month. Figure 63 shows an example from 18:00 UTC on 12 October in which the AMVs are tracking cirrus outflow from tropical storm Wipha as it strengthens to the west of the Philippines. O-B speed biases are in excess of +5 m/s across a wide area to the south of the storm system. Model best-fit pressures estimates are well constrained and indicate that the AMV assigned heights are too low by over 50 hPa. It is suspected that the height bias in the WV AMVs is due to a humidity bias in the JMA NWP model (M. Hayashi, pers comm., Feb 2012).

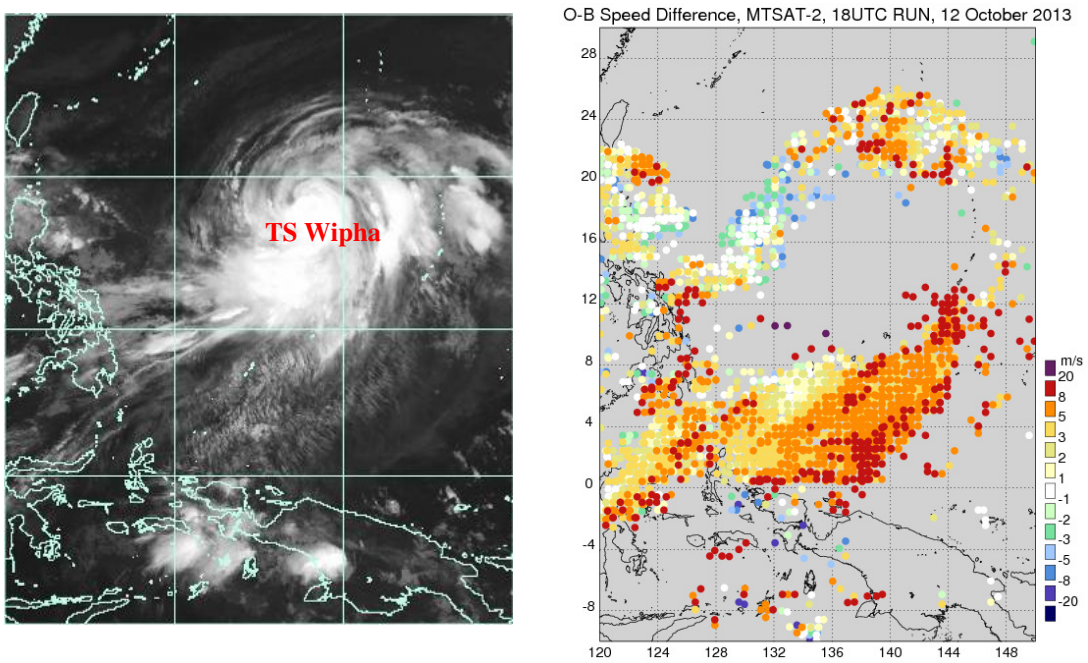


**Figure 63. MTSAT-2 IR 10.8 image at 1800 UTC 12 October 2013 (left) and a map of O-B speed bias for WV AMVs valid between 1500-2100 UTC (right).**

## Feature 6.3. Very high FY-2E WV winds

New feature:

Zonal cross sections reveal that some mixed WV channel winds from FY-2E are assigned unrealistically high heights in the atmosphere with pressures as low as 0 hPa (Figure 64). This feature seems to occur during the winter months in each hemisphere but is not seen in the equivalent plot for FY-2D which in general shows quite a different distribution (height threshold around 150 hPa). FY-2E also shows some clustering on some discrete pressure levels.

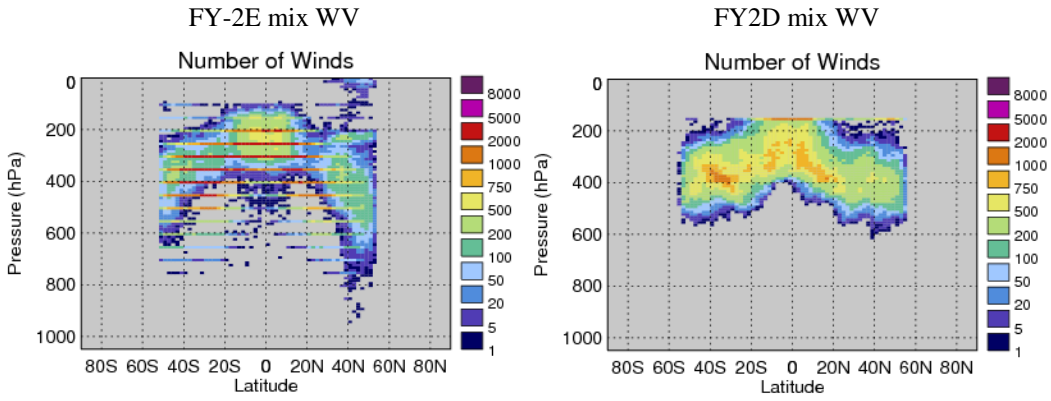


**Figure 64. Vertical distribution of FY-2E (left) and FY-2D (right) mixed WV winds from December 2012. Observations filtered for QI2 > 80.**

## 6. Polar wind updates

### Feature 6.4. EUMETSAT Metop winds near the poles

New feature:

Metop winds produced by EUMETSAT frequently show an increase in vector difference located over the poles. This is often also associated with an increase in positive speed bias. An example from September 2013 is shown in
Figure 65 where there is a spike in vector difference over the South Pole.

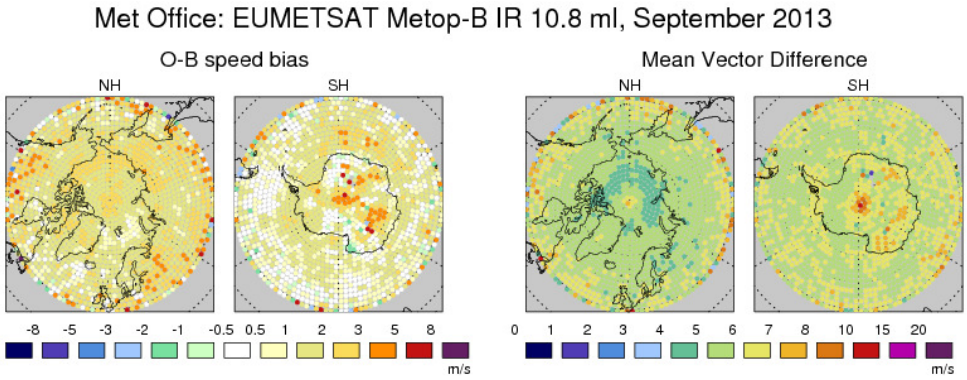


**Figure 65. Maps of speed bias and mean vector difference for EUMETSAT Metop-B AMVs in September 2013. Observations filtered for QI2 > 80 and observed pressure 400- 700 hPa.**

Comparing the EUMETSAT and CIMSS winds in the southern hemisphere for the same month reveals very different behaviour in the O-B statistics as a function of latitude (Figure 66). The EUMETSAT winds show a significant increase in RMS vector difference and speed bias pole-wards of around 86°S. The CIMSS winds tend towards a negative speed bias over the pole but show little variation in RMS vector difference. Both products have a similar number of AMVs pole-wards of 80°S. Note that binning the data this way inevitably decreases the number of observations the closer you get to the pole.

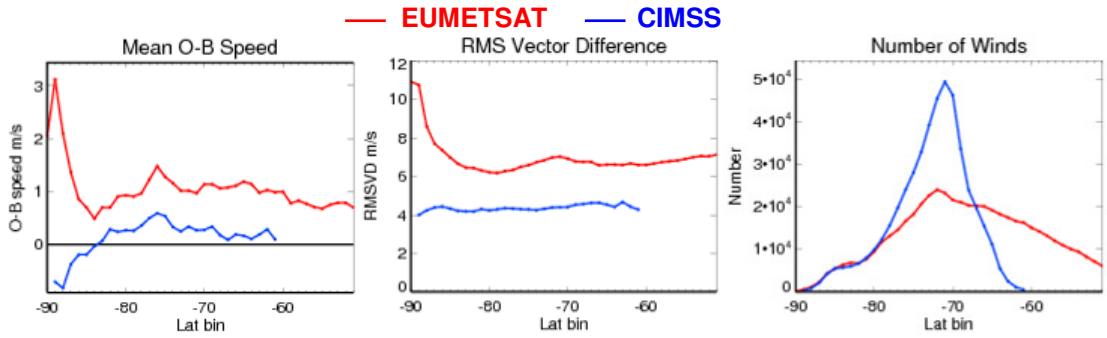


**Figure 66. Statistics as a function of latitude: speed bias, RMS vector difference and number of winds. EUMETSAT (red) and CIMSS (blue) Metop-B winds in the southern hemisphere during September 2013. Observations filtered for QI2 > 80 and observed pressure 400- 700 hPa.**

Why might the quality of the EUMETSAT winds decrease close to the poles? Figure 67 shows the same set of statistics as a function of satellite zenith angle (SZA). For the Metop image pair winds the SZA in BUFR is the value from the target (first) image and takes values from 0° at nadir to 68° at the edges of the AVHRR swath. Both speed bias and RMSVD increase with SZA, particularly beyond about 60 degrees. There is also a large spike in the mean observation speed for SZA > 60° (not shown) which rapidly doubles from 20m/s to 40 m/s between 60-68°. Figure 68 shows how the mean SZA varies spatially over the polar-regions for Metop-B AMVs. The highest mean SZA values are located around the edge of the polar disc, but also cluster around the poles. This happens because the orbit does not pass exactly over the top of the geographic poles but is inclined at an angle of 98.7° to the Equator as shown by Figure 69.

Figure 70 shows the impact of applying a SZA threshold of 50 degrees to EUMETSAT AMVs above 400 hPa. The large vector differences over the pole are reduced and the statistics around the edge of the disc are also improved.

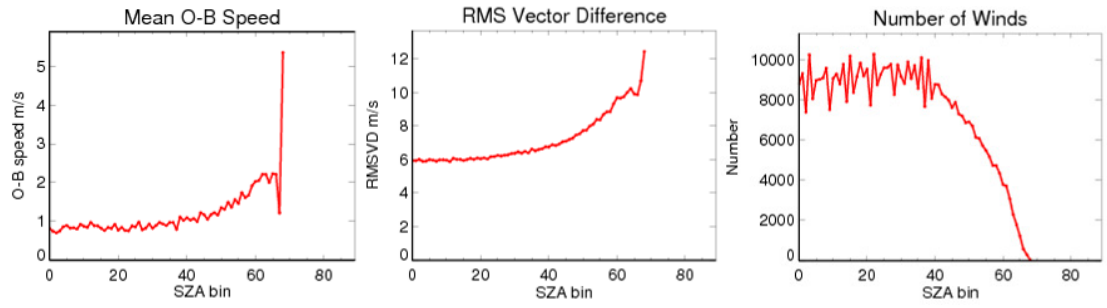


**Figure 67. Statistics as a function of SZA: speed bias, RMS vector difference and number of winds. EUMETSAT Metop-B winds in the southern hemisphere during September 2013. Observations filtered for QI2 > 80 and observed pressure 400- 700 hPa**

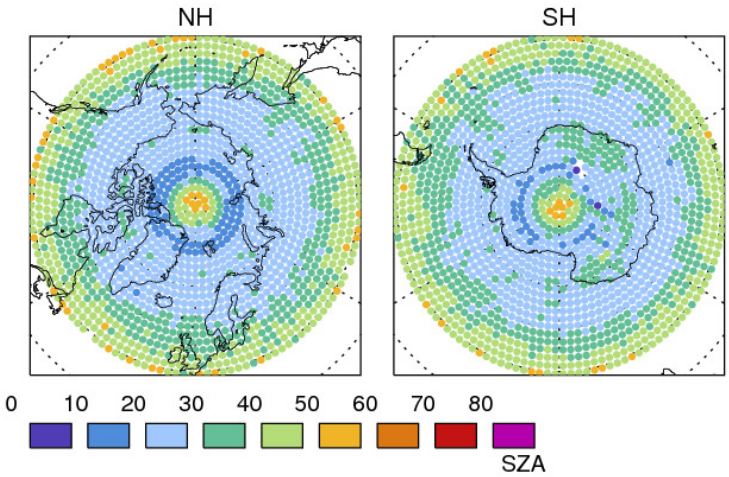


**Figure 68. As Figure 65, but showing mean satellite zenith angle.**

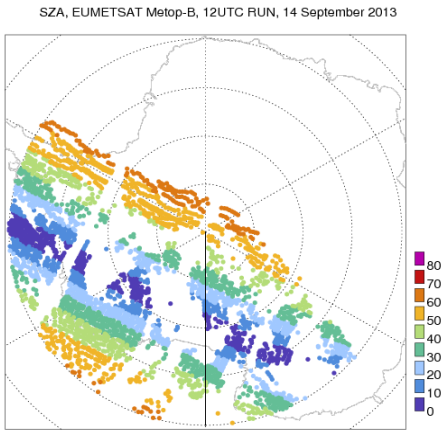


**Figure 69. Example of SZA for EUMETSAT Metop winds.**

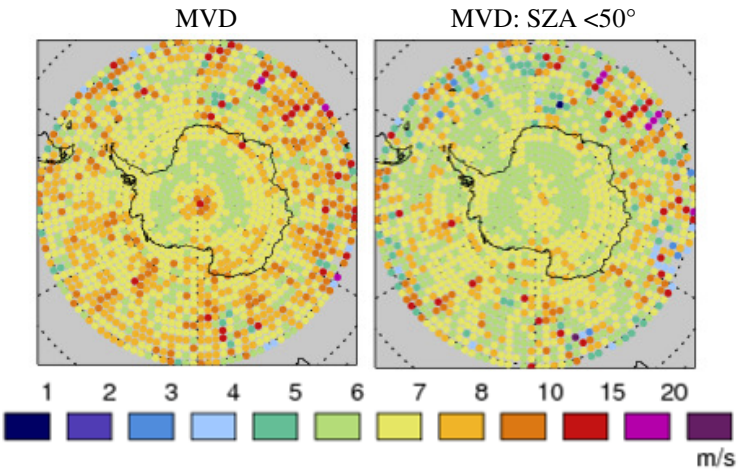


**Figure 70. Mean vector difference for EUMETSAT-produced Metop-B AMVs in September 2013: no SZA filtering (left) and SZ < 50 (right). Observations filtered for QI2 > 80 and observed pressure above 400 hPa**

## 7. Summary

The NWP SAF monitoring continues to be a valuable resource in the effort to better characterise AMV errors. Over the past two years several new data types have been added to the website including Metop-B, MSG-3, FY-2E, Kalpana-1 and LeoGeo mixed satellite winds.

The most significant change to the AMVs since AR5 has been the implementation of the CCC scheme by EUMETSAT in September 2012. This has greatly reduced the magnitude and extent of the negative speed bias at mid-high level in the extra-tropics (Features 2.9 and 2.10) which had been a growing problem for the MSG winds. Small improvements have also been noted for other features (2.6 at low level and 2.13 at high level). However the impacts at mid level are rather mixed with some worsening of the positive speed bias in the tropics. The cloudy WV channel winds in particular now show a much more widespread speed bias below 400 hPa and should be considered for blacklisting in NWP assimilation. The low level IR/VIS statistics were degraded by 20% in terms of RMSVD following the implementation of CCC, but a subsequent update has shown some improvement and so this aspect of the monitoring hasn't been covered specifically in this report.

In general the O-B statistics continue to look very similar against both the ECMWF and Met Office models. Where differences in the models do occur, AMV departures tend to be slightly more marked versus the Met Office background. The largest differences continue to be over the Pacific region (e.g. Feature 4.2) but the TEJ over N Africa is another area where the models disagree (Feature 3.2). The TEJ appears to be too strong in the Met Office model, possibly linked to errors in the larger scale monsoon circulation and could benefit from further investigation. What changes can we expect to the model in the near future? Around the middle of 2014 the Met Office global model will see its biggest upgrade in over 10 years, with a new dynamical core (ENDGame), a major upgrade to model physics and resolution increase from 25 km to 17 km at mid latitudes. This new system has been shown to significantly reduce tropospheric wind biases and improve the position of 250 hPa jet cores. This may reduce some of the biases we currently observe versus the AMVs and the ECMWF model, but this will be determined in future analysis reports.

At low level, further improvements are expected when the GOES hourly data stream becomes operational. In addition to the benefits outlined in AR5, this report has identified an improved speed bias for the GOES hourly winds over the N Atlantic

(Feature 2.3). For low level AMVs in general, the statistics are still affected by instances of large height assignment error. Examples include: tracking cirrus clouds (e.g. Feature 2.7) and non-frontal cloud in the tropics (Feature 6.1). An interesting new feature identified in this report is the bias observed between the AMVs and the models during large-scale cold air outbreaks over the east coast of the USA (Feature 2.3). The most likely error sources appear to be: 1) difficulties tracking the breakup of low level cloud as it advects across the SST front (Gulf Stream), and 2) the accuracy of the NWP forecast. A similar case was also identified near Korea/Japan (Feature 6.2).

At high level a negative speed bias has been identified for FY-2E AMVs derived over the high, cold surface of the Tibetan plateau which could benefit from further investigation. This case highlights an example where care is needed interpreting model best-fit pressure estimates due to the level of best-fit occurring close to the land surface.

## References

AR3 (2008), Forsythe, M., and R. Saunders. Third Analysis of the data displayed on the NWP SAF AMV monitoring website. Document NWPSAF-MO-TR-022.

AR4 (2010), Cotton, J., and M. Forsythe. Fourth Analysis of the data displayed on the NWP SAF AMV monitoring website. Document NWPSAF-MO-TR-024.

AR5 (2012), Cotton, J. Fifth analysis of the data displayed on the NWP SAF AMV monitoring website. Document NWPSAF-MO-TR-027.

Borde, R., Doutriaux-Boucher, M., Dew, G., and M. Carranza, (2013). A Direct Link between Feature Tracking and Height Assignment of Operational EUMETSAT Atmospheric Motion Vectors. J. Atmos. Oceanic Technol. doi:10.1175/JTECH-D-13-00126.1, in press.

Borde, R., and R. Oyama, (2008). A direct link between feature tracking and height assignment of operational atmospheric motion vectors. Proceeding from the 9th International Wind Workshop.

Cotton, J., (2013). Comparing AMVs over the Indian Ocean, Document NWPSAF-MO-TR-028, http://research.metoffice.gov.uk/research/interproj/nwpsaf/satwind_report/investigations/iodc/nwpsaf_mo_tr_028.pdf

Liu, J.W., Xie, S.P., Norris, J., and S.P. Zhang, (2014). Low-Level Cloud Response to the Gulf Stream Front in Winter using CALIPSO. Journal of Climate 2014.

Murakami, T., and B. Wang, (1993). Annual cycle of equatorial east–west circulation over the Indian and Pacific Oceans. J. Climate, **6**, 932–952.

Norris, J. R., and S. F. Iacobellis, (2005). North Pacific cloud feedbacks inferred from synoptic-scale dynamic and thermodynamic relationships. J. Clim., **18**, 4862–4878.

Webster, P. J., and J. R. Holton, (1982). Cross- equatorial response to midlatitude forcing in a zonally varying basic state. J.Atmos.Sci., **39**, 722-733

## Acknowledgements

ECMWF statistics are routinely provided thanks to Mohamed Dahoui.



MSG and MFG imagery sourced from the EUMETSAT Data Centre: http://www.eumetsat.int/website/home/Data/DataDelivery/EUMETSATDataCentre/index.html

GOES imagery sourced from the NOAA Comprehensive Large Array-data Stewardship System (CLASS): http://www.nsof.class.noaa.gov/saa/products/welcome

MODIS imagery sourced from the NASA Atmosphere Archive and Distribution System (LAADS).

FY-2E imagery courtesy of Douglas Ratcliff, SSEC Data Center, University of Wisconsin

Imagery visualised using McIDAS-X

Thanks to Pete Francis for help with the Met Office MSG cloud top pressures.